Published by Institute of Physics Publishing for SISSA/ISAS

Received: *September 18, 2004*
Accepted: *October 8, 2004*

Exact vs. semiclassical target space of the minimal string

Juan Maldacena and Nathan Seiberg

School of Natural Sciences, Institute for Advanced Study
Princeton, NJ 08540, U.S.A.
E-mail: malda@ias.edu, seiberg@ias.edu

Gregory Moore

Department of Physics, Rutgers University
Piscataway, NJ 08854, U.S.A.
E-mail: gmoore@physics.rutgers.edu

David Shih

Department of Physics, Princeton University
Princeton, NJ 08544, U.S.A.
E-mail: dshih@Princeton.edu

Abstract: We study both the classical and the quantum target space of (p, q) minimal string theory, using the FZZT brane as a probe. By thinking of the target space as the moduli space of FZZT branes, parametrized by the boundary cosmological constant x, we see that classically it consists of a Riemann surface $\mathcal{M}_{p,q}$ which is a p-sheeted cover of the complex x plane. However, we show using the dual matrix model that the exact quantum FZZT observables exhibit Stokes' phenomenon and are entire functions of x. Along the way we clarify some points about the semiclassical limit of D-brane correlation functions. The upshot is that nonperturbative effects modify the target space drastically, changing it from $\mathcal{M}_{p,q}$ to the complex x plane. To illustrate these ideas, we study in detail the example of $(p, q) = (2, 1)$, which is dual to the gaussian matrix model. Here we learn that the other sheets of the classical Riemann surface describe instantons in the effective theory on the brane. Finally, we discuss possible applications to black holes and the topological string.

Keywords: Nonperturbative Effects, D-branes, 2D Gravity, Matrix Models.

JHEP10(2004)020

Contents

JHEP10(2004)020

1. Introduction

Minimal string theories, or (p, q) minimal CFTs coupled to Liouville theory, are important examples of tractable, exactly solvable models of quantum gravity. These models are interesting laboratories for the study of string theory because, despite their simplicity, they contain many of the features of critical string theory, including D-branes, holography and open/closed duality. First solved using the dual matrix model description [1]–[8] (for reviews, see e.g. [9, 10]), recent progress in the study of Liouville theory [11]–[17] has led to a greatly improved understanding of minimal string theory from the worldsheet perspective [18]–[27].

One limitation of minimal string theory, however, has so far been the lack of a well-developed target space interpretation. In this paper, we will take the first steps towards a solution of this problem. Naively, the target space of minimal string theory is just the worldsheet Liouville field ϕ. However, it is common in string theory that different target spaces can have the same physics. In our case an equivalent description involves the free scalar field $\widetilde{\phi}$ related to ϕ by the non-local Bäcklund transformation (similar to T-duality). An important question which we will address is the distinction between the classical target space and the nonperturbative, quantum target space. We will see that they are quite different.

Our point of view (which was used among other places in [28]) is that a better effective description of target space can emerge out of the moduli space of D-branes. The advantage of this point of view is that it can capture all the nonperturbative corrections to the target space. We should point out, however, that different branes can lead to different target spaces. For example in compactification on a circle D0-branes probe the circle, while the D1-branes probe the dual circle.

Minimal string theories have D-branes (the FZZT branes) labelled by a continuous real parameter

$$x = \mu_B \tag{1.1}$$

(the boundary cosmological constant). We wish to interpret x as a target space coordinate, and the picture we have in mind is as follows. The minisuperspace wavefunction of the FZZT brane suggests that it is a D-brane in ϕ space stretching from $\phi = -\infty$ and dissolving at $\phi \sim -\frac{1}{b}\log x$ (where $b = \sqrt{\frac{p}{q}}$ is the Liouville coupling constant). Therefore, the tip of the FZZT brane at $\phi \sim -\frac{1}{b}\log x$ acts as a point-like probe of the Liouville direction.[1] It has the virtue of being able to penetrate into the strong-coupling region $\phi \to +\infty$, where one might expect there to be significant modifications to the classical target space. So in this description, target space is parametrized by the coordinate x. Large positive x corresponds to the weak-coupling region of the Liouville direction, while x of order one corresponds to strong coupling.

To see how the worldsheet dynamics of the Liouville field modifies the naive target space, it is useful to analytically continue x to complex values. In the semiclassical approximation the D-branes are not single valued as a function of x and are labelled by a point in a finite multiple cover of the x-plane. This multiple cover corresponds to a Riemann surface $\mathcal{M}$ which can be described as follows. In terms of the disk amplitude Φ we define

$$y = \partial_x \Phi \tag{1.2}$$

or equivalently

$$\Phi = \int^x y(x')dx' \,. \tag{1.3}$$

Then, x and y satisfy an algebraic equation

$$F(x, y) = 0 \tag{1.4}$$

[1] This intuition can be made more precise using the equivalent description in terms of the Bäcklund field $\widetilde{\phi}$. Here the FZZT brane corresponds to a *Dirichlet* boundary condition on $\widetilde{\phi}$ [23].

which describes the Riemann surface $\mathcal{M}$ in $\mathbb{C}^2$. The parameters of the polynomial $F(x,y)$ which determine the complex structure of $\mathcal{M}$ depend on the parameters of the minimal string. For large x and y the equation $F(x,y)=0$ becomes of the form $x^q \approx y^p$ for integer p and q. We will refer to the corresponding Riemann surface as $\mathcal{M}_{p,q}$.

Physically, what is happening is that we start probing the target space at large positive x, where the Liouville field is weakly coupled and the classical target space is a good description. Next, we bring the FZZT brane probe into the strong-coupling region x of order one, and we find a branch point at $x=-1$. This branch point is a sign that the target space is modified due to strong-coupling effects on the worldsheet. It suggests that we analytically continue into the complex x plane, through the branch cut ending at $x=-1$, and into the other sheets of the Riemann surface. Correspondingly, the moduli space of FZZT branes must be enlarged from the complex x plane to the Riemann surface $\mathcal{M}_{p,q}$. In this way, we obtain $\mathcal{M}_{p,q}$ for the semiclassical target space of the minimal string.[2]

A special situation occurs when $\mathcal{M}_{p,q}$ has genus zero. This happens for backgrounds without ZZ branes [23, 26]. Since here $\mathcal{M}_{p,q}$ has genus zero, it can be uniformized by a single complex parameter z; i.e. there is a one to one map between the complex z plane and $\mathcal{M}_{p,q}$. Then we can express the values of x and y as polynomials of degrees p and q in z

$$x = x_p(z)\,, \qquad y = y_q(z)\,. \tag{1.5}$$

The parameters in these polynomials depend on the closed string background which is labelled by the coefficients of closed string operators $t=(t_1,t_2,\ldots)$. Of particular importance among these parameters are the coefficient of the lowest dimension operator

$$\tau \equiv t_1 \tag{1.6}$$

and the worldsheet cosmological constant μ (in unitary worldsheet theories $\tau=\mu$, but in general they are different). The uniformizing parameter z has the worldsheet interpretation as the one point function on the disk of the lowest dimension operator

$$z = \partial_\tau \Phi = \partial_\tau \left(\int^x y\,dx \right)\Big|_x\,. \tag{1.7}$$

Below we will relate this expression to various points of view of the minimal string, in particular the connection to integrable hierarchies.

Most of the discussion in this paper will concern the class of backgrounds where $\mathcal{M}_{p,q}$ has genus zero. We expect our main results to apply to the more generic backgrounds with arbitrary Riemann surface and we will comment on this below.

A further useful specialization of the background is to the *conformal backgrounds* of [29]. These are backgrounds without ZZ branes in which all the closed string couplings t, with the exception of the worldsheet cosmological constant μ, have been set to

[2] It may seem strange that we started with a one dimensional target space consisting of ϕ, and we ended up with a two dimensional target space consisting of $\mathcal{M}_{p,q}$. However, the fact that all physical quantities depend holomorphically on $\mathcal{M}_{p,q}$ suggests that there is still a sense in which the target space is one dimensional.

JHEP10(2004)020

zero. In this class of theories explicit worldsheet calculations can be performed, leading to checks of the results in more general backgrounds. Here the more general expressions (1.4), (1.5) become [23] (see also [30])

$$F(x,y) = T_p\left(\frac{y}{C}\right) - T_q(x) = 0 \tag{1.8}$$

and

$$x = T_p(z)\,, \qquad y = CT_q(z)\,. \tag{1.9}$$

Here C is a normalization factor which we will determine below, $T_n(\cos\theta) = \cos(n\theta)$ is a Chebyshev polynomial of the first kind, and for simplicity we have set $\mu = 1$.

It is natural to expect that this picture of the classical target space is modified only slightly when perturbative effects in the string coupling $g_s = \hbar$ are taken into account. As we will see, however, nonperturbative effects have important consequences. To study the quantum target space, we turn in the first part of section 2 to the nonperturbative description of FZZT branes afforded by the dual matrix model. In the matrix model, FZZT branes are described by insertions of the exponentiated macroscopic loop operator [29] and [31]–[33]

$$\Psi(x) \sim e^{\mathrm{Tr}\log(x-M)} = \det(x-M) \tag{1.10}$$

into the matrix integral. We use the results of [34] to compute the correlator of any number of FZZT branes. Taking the continuum limit, we show that the correlators become

$$\left\langle \prod_{i=1}^{n} \Psi(x_i) \right\rangle = \frac{\Delta(d_j)}{\Delta(x)} \prod_{i=1}^{n} \psi(x_i, t)\,, \tag{1.11}$$

where

$$\psi(x,t) = \langle \Psi(x) \rangle \tag{1.12}$$

is the FZZT partition function, which depends on the closed-string couplings $t = t_1, t_2, \ldots$; Δ denotes the Vandermonde determinant; and d_j is shorthand for the action of $d = \hbar\partial_\tau$ on $\psi(x_j, t)$. (Note that it does *not* refer to differentiation with respect to x_j.) We argue that the denominator can be removed by thinking of the FZZT branes as wavefunctions (half-densities), with the result that the branes become fermionic.

In the classical $\hbar \to 0$ limit, we show that the FZZT correlators reduce to

$$\lim_{\hbar\to 0} \left\langle \prod_{i=1}^{n} \Psi(x_i) \right\rangle = \frac{\Delta(z)}{\Delta(x)} \prod_{i=1}^{n} \Psi_{cl}(z)\,, \tag{1.13}$$

where

$$\Psi_{cl}(z) = x'(z)^{-1/2} e^{\int^{x(z)} y(x)dx/\hbar} \tag{1.14}$$

is the semiclassical approximation to the FZZT partition function. We also provide a worldsheet interpretation for the various factors in (1.13) — the first factor $\frac{\Delta(z)}{\Delta(x)}$ comes from annulus diagrams between different FZZT branes, while the semiclassical wavefunctions

JHEP10(2004)020

$\Psi_{cl}(x_i)$ come from the disk amplitude and the annulus between the same brane. More generally, we interpret these expressions as a change in the measure of the D-branes $\Psi(x)$ to a fermion on the Riemann surface $\mathcal{M}_{p,q}$.

Using the fact that $\psi(x,t)$ is a Baker-Akhiezer function of the KP hierarchy, which is actually an *entire* function of x [35, 36], it follows that the exact FZZT correlators (1.11) are all entire functions of x. This is in spite of the fact that the classical correlators (1.13) are clearly functions on $\mathcal{M}_{p,q}$. Evidently, the quantum target space differs significantly from the classical target space. Whereas the latter comprised the Riemann surface $\mathcal{M}_{p,q}$, the former consists of only the complex x plane!

In section 2.4, we analyze additional FZZT observables (the quantum resolvents) and show that they are also entire functions of x. Finally, we rederive the WKB approximation (1.14) using the fact that $\psi(x,t)$ is a Baker-Akhiezer function. We note that the asymptotics exhibit "level crossing" behavior at large negative x. Here, by level crossing we mean simply that there is a branch cut along the negative real axis with different values of $\psi(x,t)$ above and below the cut. Below, when this approximation of $\psi(x,t)$ will be associated with saddle points in an integral, we will see that two saddle points exchange dominance there.

In section 3, we illustrate our general arguments with the simplest example of minimal string theory, namely the topological $(p,q) = (2,1)$ model. This is dual to the gaussian matrix model, and we show that the FZZT partition function is expressed in terms of the Airy function. By representing the insertion of a D-brane as a Grassmann integral in the matrix model, we give a direct and simple proof of the equivalence between the $n \times n$ Kontsevich model and the double-scaled $(2,1)$ model with n FZZT branes. That is, we show that in the continuum double scaling limit

$$\left\langle \prod_{i=1}^{n} \Psi(x_i) \right\rangle \to \int dS \; e^{\mathrm{Tr}\left(iS^3/3 + i\hbar^{-2/3}(X+\tau)S\right)} \tag{1.15}$$

with S and X $n \times n$ hermitean matrices and τ, which can be absorbed in X, is the coupling constant of the theory. The eigenvalues of X are $x_1, \ldots, x_n$ after an appropriate shift and rescaling in the double scaling limit (see below). Using this approach, we see very directly how the matrix S of the $n \times n$ Kontsevich model is the effective degree of freedom describing open strings stretched between n FZZT branes [24].

We continue our study of the $(2,1)$ model in section 4, focusing now on the effective theory on the FZZT brane, which is described by the Airy integral (1.15) with $n = 1$. An analysis of this integral using the stationary phase method reveals several new facts. To begin, we show how the other sheets of the classical moduli space can be viewed as saddle points in the integral describing the FZZT partition function. Therefore, they can be thought of as instantons in the effective theory on the brane. We expect this conclusion to hold for all values of (p,q).

A more careful stationary phase analysis of the Airy integral illustrates the general mechanism by which the target space is modified nonperturbatively. Exponentially small quantities — neglected in perturbative string theory — can become large upon analytic continuation, and these large corrections "erase" the branch cuts and monodromies of the Riemann surface in the exact answer. The essence of the replacement of the semiclassical target space $\mathcal{M}_{p,q}$ by the humble complex x-plane is thus what is known as Stokes' phenomenon. Generally speaking, Stokes' phenomenon is the fundamental fact that the analytic continuation of an asymptotic expansion can differ from the asymptotic expansion of an analytic continuation. In our case, the Riemann surface is extracted by working in the classical approximation to string theory (thus taking the leading term in an asymptotic expansion in $g_s = \hbar$) and then considering the analytic continuation. Thus, the Riemann surface arises from the analytic continuation of the asymptotics. Thanks to the matrix model we can study the analytic continuation of the exact nonperturbative answers for amplitudes directly. The fact that the FZZT amplitudes are entire shows that the Riemann surface "disappears" nonperturbatively.

In terms of the saddle point analysis of the field theory living on the FZZT branes, Stokes' phenomenon is exhibited in two ways. The first, more trivial way, occurs when the parameter x is varied across what is known as an *anti-Stokes' line*. This can be thought of as a first-order phase transition where two contributing saddle points exchange dominance. The story is incomplete, however, if we simply consider only the anti-Stokes' lines. In addition, there is also a more subtle phenomenon happening along what are called *Stokes' lines*. As x is varied across a Stokes' line, a subdominant saddle abruptly ceases to contribute to the exact answer. This phenomenon is most dramatic when we continue to vary x and the missing saddle becomes the *dominant* saddle, even though it is still not contributing to the integral. In terms of the path integral describing the effective theory on the brane, what is happening is that one simply cannot deform the contour of integration to pass through that saddle. We will discuss this in more detail in appendix B.

In section 5, we comment on the issues involved in generalizing to other backgrounds. Among other things, we show using the FZZT partition function that not all values of (p, q) correspond to nonperturbatively consistent backgrounds with a double-scaled matrix model that is bounded from below. We deduce a bound

$$\sin \frac{\pi q}{p} > 0 \tag{1.16}$$

that must be satisfied in order for the corresponding background to exist. For instance, when $p = 2$ only the $(p, q) = (2, 2m-1)$ models with m odd exist nonperturbatively, while the models based on the unitary discrete series with $q = p + 1$ never exist nonperturbatively.

Finally, section 6 contains a possible analogy with the work of [37] on the physics behind black hole horizons and possible implications for the topological string approach of [38]. In appendix A, we review the Lax formalism of minimal string theory (the operators P and Q and the string equation $[P, Q] = \hbar$), and we present new results concerning the geometrical interpretation of its classical limit. Appendix B, as mentioned above, contains a brief review of Stokes' phenomenon along the lines of [39], while appendix C contains the results of a numerical analysis of $(p, q) = (2, 5)$.

2. The Quantum Target Space: FZZT Branes in the Matrix Model

2.1 FZZT correlators at finite N

As is well-known, (p, q) minimal string theory possesses a dual matrix model description. For $p = 2$, the dual matrix model consists of an $N \times N$ hermitean matrix M with potential $V(M)$ and coupling g,

$$\mathcal{Z}(g) = \int dM \; e^{-\frac{1}{g}\operatorname{Tr} V(M)} \tag{2.1}$$

while for $p > 2$ one needs to use an analogously defined two-matrix model (for recent discussion of the two-matrix model and references, see [40]):

$$\widetilde{\mathcal{Z}}(g) = \int dM d\widetilde{M} \; e^{-\frac{1}{g}\left(\operatorname{Tr} V(M) + \operatorname{Tr} W(\widetilde{M}) - \operatorname{Tr} M\widetilde{M}\right)}. \tag{2.2}$$

Here the measures dM and $d\widetilde{M}$ include a factor of the volume of $\mathrm{U}(N)$.

In the matrix model, macroscopic loops are created by insertions of the operator

$$W(x) = \frac{1}{N} \operatorname{Tr} \log(x - M) \tag{2.3}$$

in the matrix integral.[3] For instance, the large N limit of $\langle W(x) \rangle$ corresponds to the FZZT disk amplitude Φ (up to a polynomial in x), and the matrix model resolvent

$$R(x) = \partial_x \langle W(x) \rangle = \frac{1}{N} \left\langle \operatorname{Tr} \frac{1}{x - M} \right\rangle \tag{2.4}$$

corresponds to $y(x)$ (again up to a polynomial in x).

The full FZZT brane obviously does not correspond to a single macroscopic loop in the worldsheet. Rather, we must include contributions from worldsheets with any number of boundaries. This is accomplished by exponentiating $W(x)$, whereby the full, nonperturbative FZZT brane is represented by a determinant operator

$$e^{NW(x)} = \det(x - M) \tag{2.5}$$

in the matrix model. We can also write this determinant as a Grassmann integral over N complex fermions χ_i

$$\det(x - M) = \int d\chi d\chi^\dagger e^{\chi^\dagger (x-M)\chi} \, . \tag{2.6}$$

In [18]–[21] and [26], the matrix M of the one-matrix model was interpreted as describing the (bosonic) open strings stretched between the N condensed ZZ branes in the Fermi sea. Meanwhile, the χ_i are taken to represent *fermionic* open strings stretched between the FZZT brane and the N ZZ branes [26]. Now consider the correlation function of any number of FZZT branes, which nonperturbatively is given by a product of determinants. Amazingly, this can be explicitly evaluated in both the one and two matrix models [34].

[3] In the two-matrix model, there is another loop made out of $\widetilde{M}$. It corresponds to the "dual" FZZT brane and classically is related to the loop (2.3) by a Legendre-type transform [40]. We will discuss the interpretation of this dual loop in section 6.

The answer is

$$\left\langle \prod_{i=1}^{n} \det(x_i - M) \right\rangle = \frac{\det(P_{N+i-1}(x_j))}{\Delta(x)} \,. \tag{2.7}$$

Here $\Delta(x) = \prod_{i<j}(x_i - x_j)$ is the Vandermonde determinant, $P_k(x)$ are the orthogonal polynomials of the matrix model (or bi-orthogonal polynomials associated to M in the two-matrix model) with leading coefficient 1, and the indices i and j in (2.7) run between 1 and n. The simplest case of the general formula (2.7) is the FZZT partition function. This is given by a single orthogonal polynomial:

$$\langle \det(x - M) \rangle = P_N(x) \tag{2.8}$$

Below, we will take the continuum limits of (2.7) and (2.8), and we will see how the perturbative loop correlators can be recovered.

Before we proceed, let us briefly mention an interpretation of the FZZT correlator (2.7) that will be useful in the next subsection. First, we need to write the l.h.s. of (2.7) more compactly in the following way

$$\left\langle \prod_{i=1}^{n} \det(x_i - M) \right\rangle = \langle \det(X \otimes I_N - I_n \otimes M) \rangle \,, \tag{2.9}$$

where I_N and I_n denote the $N \times N$ and $n \times n$ identity matrices respectively, and X is understood to be an $n \times n$ hermitean matrix with eigenvalues $x_1, \ldots, x_n$. Now notice that if we square $\det(X \otimes I_N - I_n \otimes M)$, multiply by $e^{-\frac{1}{g}(\mathrm{Tr}\, V(M) + \mathrm{Tr}\, V(X))}$, and integrate over X and M, we obtain the $(N+n) \times (N+n)$ matrix integral with no insertions of FZZT branes, i.e.

$$\int dX dM \; e^{-\frac{1}{g}(\mathrm{Tr}\, V(M) + \mathrm{Tr}\, V(X))} \det(X \otimes I_N - I_n \otimes M)^2 = \int d\widehat{M} \; e^{-\frac{1}{g}\mathrm{Tr}\, V(\widehat{M})} \,, \tag{2.10}$$

where $\widehat{M}$ is an $(N+n) \times (N+n)$ hermitean matrix. (As before, the integration measures include factors of the volume of the relevant unitary group.) The meaning of (2.10) is that the FZZT creation operator $\det(X \otimes I_N - I_n \otimes M)$ acts as a kind of wavefunction (half-density) on the space of hermitean matrices X.

The motivation for interpreting $\det(X \otimes I_N - I_n \otimes M)$ as a wavefunction in X-space is that it allows us to think of the FZZT branes as fermions. To see this, recall that the measure for an integral in X space is

$$dX = dU \prod_{i=1}^{n} dx_i \; \Delta(x)^2 \,, \tag{2.11}$$

where U is an $n \times n$ unitary matrix (and the measure is such that $\int dU = 1$). Hence, a half-density $(dX)^{1/2}$ carries with it a factor of $\Delta(x)$, which is precisely what is needed to cancel the denominator of (2.7).[4] (Put differently, the factor $\Delta(x)$ plays a role analogous

[4]The annulus diagram is the logarithm of the $n = 2$ version of (2.7). In [26], where this diagram was calculated, it was pointed out that the term associated with the denominator of (2.7) is independent of the coupling constants and therefore could be removed. Here we see a more geometric way of deriving this fact.

JHEP10(2004)020

to that of cocycles in vertex operator algebra theory, by enforcing the correct statistics of the determinant operator.) This leaves the numerator of (2.7), which is obviously antisymmetric under interchange of the x_i's. Therefore, the FZZT branes become fermionic.

2.2 FZZT correlators in the continuum limit

Now let us take the large N double-scaling limit of (2.7) to obtain the D-brane correlators of minimal string theory. For simplicity, we start with the $n = 1$ case (2.8). As in (2.10), to have a well-defined scaling limit we must consider not the determinant, but rather the following operator [35, 9]

$$\Psi(x) = \frac{1}{\sqrt{h_N}} e^{-V(x)/2g} \det(x - M)\,, \tag{2.12}$$

where $V(x)$ is the matrix model potential, and h_N is a normalizing constant. (Some rigorous results on the double-scaled limit of the orthonormal wavefunctions have been derived in [41].) This converts the orthogonal polynomials in (2.7) to orthonormal wavefunctions with measure dx. Then the FZZT partition function in the double-scaling limit is given by a function of x and the background closed-string couplings $t = (t_1, t_2, \ldots)$,

$$\langle \Psi(x) \rangle = \psi(x, t) \tag{2.13}$$

which is characterized by the requirement that it satisfy the differential equations

$$Q\psi(x,t) = x\psi(x,t), \qquad P\psi(x,t) = \hbar\partial_x\psi(x,t) \tag{2.14}$$

with $P \propto d^q + \ldots$ and $Q \propto d^p + \ldots$ differential operators in $d = \hbar\partial_\tau$.[5] (Note that the derivative d is taken at fixed values of $x, t_{j>1}$.) P and Q are known as Lax operators, and they are determined by the string equation

$$[P, Q] = \hbar \tag{2.15}$$

In appendix A, we review the properties of P and Q and present new results concerning the geometric interpretation of these operators in the classical limit. For a more pedagogical introduction to the Lax formalism and integrable hierarchies, see e.g. [10, 42].

Note that the differential equations (2.14) do not specify $\psi(x, t)$ uniquely. In nonperturbatively consistent models, we will see below that this ambiguity can be completely fixed, in part by the boundary condition that $\psi(x, t)$ be real and exponentially decreasing as $x \to +\infty$.

In the literature on integrable systems, the function $\psi(x, t)$ is referred to as the "Baker-Akhiezer function" of the associated KP hierarchy defined by P and Q. Here we see that it has a simple, physical interpretation in minimal string theory as the FZZT partition function. For our present purposes, the most important property of the Baker-Akhiezer

[5] It is common in the literature to denote the lowest dimension coupling by x. We denote it here by τ.

function is the non-trivial fact that it (along with all of its derivatives) is an *entire function* of x.[6] We will see momentarily that this has dramatic consequences for the quantum moduli space of FZZT branes.

In the double-scaling limit, it is not difficult to show that the general FZZT correlator (2.7) becomes

$$\left\langle \prod_{i=1}^{n} \Psi(x_i) \right\rangle = \frac{\Delta(d_j)}{\Delta(x)} \prod_{i=1}^{n} \psi(x_i, t)\,, \tag{2.16}$$

where the notation d_j is shorthand for the action of $d = \hbar\partial_\tau$ on $\psi(x_j, t)$. To derive (2.16) use the fact that the increase of index on P_k becomes a derivative with respect to τ to leading order in the double-scaling parameter ϵ. Then as $\epsilon \to 0$, only the Vandermonde determinant of derivatives with respect to the index survives. We conclude from (2.16) that the correlator of any number of FZZT branes reduces, in the continuum limit, to a product of Baker-Akhiezer functions $\psi(x_i, t)$ and their derivatives.

2.3 Comparison with the semiclassical limit

Having obtained the exact D-brane correlators (2.16), it is straightforward to take their semiclassical limit and show how the perturbative loop amplitudes can be recovered. For this, we will need a result from subsection 2.5, namely that as $\hbar \to 0$, the Baker-Akhiezer function becomes an eigenfunction of d with eigenvalue z. (As discussed in the introduction, the global uniformizing parameter z exists only in the backgrounds without ZZ branes.) Therefore, the semiclassical limit of (2.16) is simply

$$\lim_{\hbar\to 0} \left\langle \prod_{i=1}^{n} \Psi(x_i) \right\rangle = \frac{\Delta(z)}{\Delta(x)} \prod_{i=1}^{n} \Psi_{cl}(z_i)\,. \tag{2.17}$$

The worldsheet description of the various terms appearing in (2.17) is as follows. Recall that we can think of the FZZT creation operator $\Psi(x) \sim e^{W(x)/\hbar}$ as the exponentiated macroscopic loop operator. Then the first factor $\frac{\Delta(z)}{\Delta(x)}$ is the exponentiated contribution of the annulus diagrams with the ends of the annulus ending on different branes. This is consistent with the explicit worldsheet calculation in conformal backgrounds which leads to the connected annulus amplitude [26]

$$\langle W(x)W(x')\rangle_{\mathrm{c,\,ann}} = \log\left(\frac{z-z'}{x-x'}\right). \tag{2.18}$$

The other diagrams that contribute at this order in $\hbar$ are the disk diagram (1.3) and the annulus diagram with the two ends on the same brane[7]

$$\lim_{x'\to x} \frac{1}{2}\langle W(x)W(x')\rangle_{\mathrm{c,\,ann}} = \lim_{z'\to z} \frac{1}{2}\log\left(\frac{z-z'}{x(z)-x(z')}\right) = -\frac{1}{2}\log \partial_z x(z). \tag{2.19}$$

[6] This fact was proven in [35, 36] by writing the string equation in an equivalent form as an equation for a *flat* holomorphic vector bundle on the space of x, t_k. The connection on this vector bundle is polynomial in x. The Baker-Akhiezer function is used to make a covariantly constant frame. From the equation $(\frac{d}{dx} - A_x)\widetilde{\Psi} = 0$, where $\widetilde{\Psi}$ is the frame, it follows, via the path-ordered exponential, that $\widetilde{\Psi}$ is entire in x.

[7] The factor of a half comes from the fact that the open strings are ending on the same brane.

These diagrams combine to give the WKB wave functions in (2.17):

$$\begin{aligned}
\Psi_{cl}(z) &= f(z)e^{\Phi(z)/\hbar} \\
\Phi(z) &= \int^{x(z)} y dx \\
f(z) &= \frac{1}{\sqrt{\partial_z x(z)}} \,.
\end{aligned} \tag{2.20}$$

As is common in WKB wavefunctions, the prefactor $f(z)$ is a one loop correction. In our case it arises from an open string loop which is the annulus diagram. Finally, note that higher genus diagrams are suppressed in the $\hbar \to 0$ limit in (2.17).[8]

The difference between the classical result (2.17) and the exact quantum result (2.16) is at the heart of our analysis. The classical answer is obviously defined on a multiple cover of the complex x plane, since for the same x, there can be p different values of z. On the other hand, since $\psi(x,t)$ and its τ derivatives are entire functions of x, the exact expressions (2.16) for the FZZT correlators are actually entire in the complex x plane. In other words, there are no branch cuts or other singularities that necessitate analytic continuation to other sheets. Apparently, the semiclassical target space $\mathcal{M}_{p,q}$ disappears when one takes nonperturbative effects into account!

In the next subsection, we will check our picture of the quantum target space by computing the quantum resolvent and showing that it is also an entire function of x. However, we would like to first mention another perspective on the semiclassical correlator (2.17) and how this is modified in the exact answer. Recall that the FZZT brane could be thought of as a half density multiplied by $(dx)^{1/2}$. Thus the annulus factor $f(z)$ can be interpreted as a measure factor implementing a transformation from x to z. By the same token, we can think of the correlator of n FZZT branes as a half-density multiplied by $(dX)^{1/2}$ where X is an $n \times n$ matrix with eigenvalues x_i (see (2.11)). Then the transformation of this half-density to Z-space, with Z an $n \times n$ matrix whose eigenvalues are z_i, must include a factor of the jacobian

$$\left| \frac{\partial Z}{\partial X} \right|^{1/2} = \frac{\Delta(z)}{\Delta(x)} \prod_{i=1}^{n} f(z_i) \,. \tag{2.21}$$

But according to the discussion above, this is precisely the contribution of the annulus to the correlator! Thus we have shown that

$$\lim_{\hbar \to 0} \left\langle \prod_{i=1}^{n} \Psi(x_i) \right\rangle (dX)^{1/2} = e^{\mathrm{Tr}\ \Phi(Z)} (dZ)^{1/2} \tag{2.22}$$

with $\Phi(z)$ as in (2.20). Evidently, the classical correlators reduce to extremely simple expressions in z-space.

[8] We would like to stress that the leading order expressions (2.17), (2.20) are correct in any background without ZZ branes and not only in the conformal backgrounds. The only fact that is needed is that the Riemann surface $\mathcal{M}_{p,q}$ can be uniformized by the complex parameter z; i.e. that it has genus zero. We will return to this WKB wavefunction in section 2.5.

These simple expressions suggest there should be an equally simple formalism underlying the classical theory. One possibility was alluded to above, namely that instead of thinking of these correlators as half densities we can equivalently think of them as fermions. Then (2.22) indicates that *in the semi-classical limit*, there is a sense in which the FZZT branes are actually fermions on the Riemann surface $\mathcal{M}_{p,q}$. (Remember that the z plane covers $\mathcal{M}_{p,q}$ exactly once.) Such fermions are common in the matrix model literature (for reviews, see e.g. [9, 34, 42, 43]). However, our general discussion suggests that this simple picture cannot be correct in the full nonperturbative theory, in which the Riemann surface $\mathcal{M}_{p,q}$ is replaced by the complex x plane. We return to this point at the end of section 6.

2.4 The analytic structure of the quantum resolvent

Although we have shown that physical observables involving the determinant operator are entire functions of x, it remains to be seen whether the same is true for the resolvent $R(x)$ defined in (2.4). To all orders in $\hbar$ the resolvent is expected to exhibit monodromy and have various branch cuts in the complex x plane. But in the dual string theory, the resolvent (or rather its integral) corresponds to the vacuum amplitude of a worldsheet with one boundary and an arbitrary number of handles. Thus we might expect that nonperturbative effects drastically modify the classical resolvent, just as they modified the classical determinant correlators (2.17).

For simplicity, we will limit ourselves to the one-matrix model, which describes the theories with $p = 2$. Then the matrix integral defining the resolvent can be easily reduced, using the determinant formula (2.7), to a single integral in terms of orthogonal polynomials:

$$R(x) = \int_{-\infty}^{\infty} \frac{\rho_N(\lambda)}{x-\lambda}\,, \tag{2.23}$$

where

$$\rho_N(\lambda) = \frac{1}{N}\sqrt{\frac{h_N}{h_{N-1}}}\left(\psi_{N-1}(\lambda)\psi'_N(\lambda) - \psi'_{N-1}(\lambda)\psi_N(\lambda)\right) \tag{2.24}$$

with $\psi_k(\lambda) = \frac{1}{\sqrt{h_k}} e^{-V(\lambda)/2g} P_k(\lambda)$ the orthonormal wavefunctions of the matrix model and $\psi' = \frac{d}{d\lambda}\psi$. As we discussed above, $\psi_N(\lambda)$ becomes the Baker-Akhiezer function $\psi(\lambda, t)$ in the double-scaling limit. Then the exact, double-scaled resolvent is[9]

$$R(x) = \int_{-\infty}^{\infty} \frac{\rho_\hbar(\lambda)}{x-\lambda} \tag{2.25}$$

with

$$\rho_\hbar(\lambda) = A\hbar^2\left(\partial_\tau\psi(\lambda,t)\partial_\lambda\psi(\lambda,t) - \psi(\lambda,t)\partial_\tau\partial_\lambda\psi(\lambda,t)\right), \tag{2.26}$$

where A denotes some overall numerical factor which will be irrelevant for our purposes, and τ corresponds to the lowest-dimension coupling as below (2.14). From the expression for the double-scaled resolvent, it is clear that we can think of $\rho_\hbar(\lambda)$ as defining the quantum eigenvalue density.

[9] As is usual when defining the continuum resolvent, one might have to impose a cutoff on the integral at $-\Lambda$; this does not affect the arguments below.

Since the Baker-Akhiezer function is an entire function of λ, the resolvent will be everywhere analytic, except along the real axis, where it suffers from a discontinuity

$$R(x+i\epsilon) - R(x-i\epsilon) = 2\pi i \rho_\hbar(x), \qquad x \in \mathbb{R}. \tag{2.27}$$

Contrast this with the classical resolvent, which is discontinuous only along a semi-infinite cut. The discontinuity (2.27) suggests that we define two resolvents, $R_+(x)$ and $R_-(x)$, which are obtained by analytically continuing $R(x)$ through the real axis from either the upper half plane or the lower half plane, respectively. Explicitly, we define

$$R_\pm(x) = \int_{C_\pm} \frac{\rho_\hbar(\lambda)}{x-\lambda}, \tag{2.28}$$

where the contour C_+ (C_-) travels below (above) x and satisfies the same boundary conditions at infinity as the original contour in (2.25). Then we have

$$R(x) = \begin{cases} R_+(x) & \text{for Im x} > 0 \\ R_-(x) & \text{for Im x} < 0 \end{cases} \tag{2.29}$$

and also

$$R_+(x) - R_-(x) = 2\pi i \rho_\hbar(x) \tag{2.30}$$

for all $x \in \mathbb{C}$. Given the definition (2.28), it is clear that both $R_\pm(x)$ are entire functions of x.

Finally, let us consider the classical limit $\hbar \to 0$. In this limit, the resolvent must reduce to the classical resolvent, which solves the factorized loop equation and has a semi-infinite branch cut along the real x axis. Therefore, according to (2.29), $R_+(x)$ has the correct classical limit for $\mathrm{Im}\, x > 0$, while $R_-(x)$ has the correct classical limit for $\mathrm{Im}\, x < 0$. Analytically continuing the classical limits of either $R_+(x)$ or $R_-(x)$, we find the branch cut and the second sheet of the Riemann surface. Note that it is essential *first* to take the classical limit (i.e. drop the nonperturbative corrections), and only then to analytically continue the resolvent. Otherwise, we will not find the second sheet, since $R_\pm(x)$ are both entire functions of x.

To summarize, we have seen that it is impossible to define globally the quantum resolvent $R(x)$, due to the discontinuity on the real x axis. Instead, we can define through analytic continuation *two* resolvents $R_\pm(x)$, both of which are entire in the complex plane. So for the resolvent, just as for the determinant, the Riemann surface disappears at $\hbar \neq 0$ and is replaced with the complex plane. To recover the Riemann surface, we must *first* take the classical limit of the resolvents, and *then* analytically continue.

2.5 More on the FZZT partition function

We have seen above how in the double-scaling limit, all of the observables involving the FZZT brane reduce to products, derivatives, and integrals of a single quantity, the FZZT partition function $\psi(x,t)$. Thus it makes sense to study this object in more detail. Although we do not have a general formula for $\psi(x,t)$ (see below however, where we study the example of the gaussian matrix model), we extracted its asymptotic behavior at small $\hbar$ in (2.20) using worldsheet methods. Here we would like to rederive the WKB approximation

$$\psi \approx \Psi_{cl}(z,t) = (\partial_z x(z,t))^{-1/2} e^{\int_{x_0}^{x(z,t)} y(x,t)dx/\hbar} \tag{2.31}$$

starting from a completely different point of view, namely the fact that the FZZT partition function is a Baker-Akhiezer function of the KP hierarchy. We must demonstrate that (2.31) satisfies (2.14) in the $\hbar \to 0$ limit. This was first shown in [36] for $p = 2$ (together with the interpretation in terms of Riemann surfaces). We now give a simpler, but equally rigorous, proof of this result.

The first step in the proof is to act on Ψ_{cl} with $d = \hbar\partial_\tau$ (at fixed x). To leading order in $\hbar$, this gives

$$\frac{d\Psi_{cl}}{\Psi_{cl}} = \int_{x_0}^{x} \partial_\tau y|_x dx + \mathcal{O}(\hbar)\,. \tag{2.32}$$

We can simplify this by writing $y = y(x(z,t),t)$ and converting the derivative at fixed x to one at fixed z:

$$\begin{aligned}\int_{x_0}^{x} \partial_\tau y|_x dx &= \int_{x_0}^{x} \left(\partial_\tau y|_z - \partial_x y|_\tau \partial_\tau x|_z\right) dx \\ &= \int_{z_0}^{z} \left(\partial_\tau y|_z \partial_z x|_\tau - \partial_z y|_\tau \partial_\tau x|_z\right) dz\,,\end{aligned} \tag{2.33}$$

where we have used $\partial_z y|_\tau = \partial_x y|_\tau \partial_z x|_\tau$ in the second equation. We recognize the integrand in the second equation to be the Poisson bracket of x and y. Using the freedom to shift $z_0 \to 0$, together with the fact that x and y are given by

$$x(z,\tau) = Q(d=z,\tau)|_{\hbar=0}\,, \qquad y(z,\tau) = P(d=z,\tau)|_{\hbar=0} \tag{2.34}$$

and must therefore satisfy the genus zero string equation

$$\{x,y\} = \partial_\tau x \partial_z y - \partial_\tau y \partial_z x = 1 \tag{2.35}$$

(see appendix A for a proof of this), we conclude that

$$\int_{x_0}^{x} \partial_\tau y|_x dx = z\,. \tag{2.36}$$

Using (2.36) in (2.32) we readily see that the classical Baker-Akhiezer function Ψ_{cl} is an eigenfunction of d with eigenvalue z in the classical $\hbar \to 0$ limit. Note that, as mentioned in the introduction, this identity can also be proven using worldsheet techniques for the special case of the conformal background [23]. The advantage of the derivation we have given here is that it is valid in every background where the uniformizing parameter z exists (i.e. backgrounds without ZZ branes, in which case $\mathcal{M}_{p,q}$ has genus zero).

At the next order in $\hbar$ we need to consider several terms. The first step is to expand the operators $Q = Q_0 + \hbar Q_1 + \cdots$, and $P = P_0 + \hbar P_1 + \cdots$, where all derivatives are on the right hand side. In appendix A, we show that

$$Q_1 = \frac{1}{2}\partial_\tau\partial_z x|_{z=d}, \qquad P_1 = \frac{1}{2}\partial_\tau\partial_z y|_{z=d}\,, \tag{2.37}$$

where $x(z,\tau)$ and $y(z,\tau)$ are the classical expressions (2.34). (Except when specified explicitly, the derivatives of x are taken when $x(z,\tau)$ is considered as a function of z and τ. Thus ∂_τ here is taken at fixed $z, t_{j>1}$.) When d acts on the exponent of the wavefunction (2.31) it gives back z as in (2.36). In addition, we need to consider two more terms at this order in $\hbar$. The first contribution arises from a second derivative of the exponent. This gives a term of the form

$$\frac{1}{2}\partial_z^2 x \; (\partial_\tau z|_x)\,, \tag{2.38}$$

where the factor of $\frac{1}{2}\partial_z^2 x$ comes from selecting the two derivatives in Q_0 which are acting twice on the exponent of the wavefunction, and then evaluating the rest of the derivatives using the classical result. The second term appears when the derivatives of Q act on the prefactor of (2.31). This leads to a term of the form

$$-\frac{1}{2}\partial_z x \;\; \partial_\tau \left(\log \partial_z x|_\tau\right)|_x \;, \tag{2.39}$$

where again the factor $\partial_z x$ selects the derivative in Q_0 that is acting on the prefactor of (2.31) . So finally we obtain that

$$(Q-x)\Psi_{cl} = \hbar\left(\frac{1}{2}\partial_z^2 x\,\partial_\tau z|_x - \frac{1}{2}\partial_z x \;\; \partial_\tau\left(\log\partial_z x|_\tau\right)|_x + Q_1\right)\Psi_{cl} + \mathcal{O}(\hbar^2)\,. \tag{2.40}$$

We now use $\partial_\tau z|_x = -\frac{\partial_\tau x}{\partial_z x}$ to simplify these terms. In particular, we have

$$\partial_\tau\left(\log\partial_z x|_\tau\right)|_x = \frac{\partial_\tau\partial_z x + \partial_z^2 x\partial_\tau z|_x}{\partial_z x} = \frac{\partial_z x\partial_\tau\partial_z x - \partial_z^2 x\partial_\tau x}{(\partial_z x)^2}\,. \tag{2.41}$$

Then using (2.41) and (2.37) we find that all terms of order $\hbar$ in (2.40) cancel.

Computing the action of P on Ψ_{cl} takes a little more work. Using again the results above, one can show that

$$(P-\hbar\partial_x)\Psi_{cl} = \frac{1}{2}\hbar\left(\frac{\partial_z\partial_\tau y\partial_z x - \partial_z^2 y\partial_\tau x - \partial_z y\partial_z\partial_\tau x}{\partial_z x} + \frac{\partial_z^2 x(\partial_z y\partial_\tau x - 1)}{(\partial_z x)^2}\right)\Psi_{cl} + \mathcal{O}(\hbar^2)\,. \tag{2.42}$$

By applying the genus zero string equation (2.35) and its derivative with respect to z, we see that the terms in parentheses all cancel, confirming that

$$P\Psi_{cl} = \hbar\partial_x\Psi_{cl} + \mathcal{O}(\hbar^2)\,. \tag{2.43}$$

This completes our proof that Ψ_{cl} is indeed the leading-order WKB approximation to the Baker-Akhiezer function.

Let us also offer the following non-trivial consistency check of the semiclassical approximation (2.31). This approximation clearly suffers from a p-fold ambiguity, corresponding to which branch of $y(x)$ and which value of z in $x'(z)$ we choose. The correct branch is chosen at large positive x by demanding that $y(x)$ be given by its physical sheet as $x \to +\infty$. For large $|x|$ in the first sheet we have

$$y \approx 2^{\frac{q}{p}-1} C x^{\frac{q}{p}}\,, \tag{2.44}$$

where the real constant C was determined in [26]. Its sign is

$$\eta \equiv \mathrm{sign}(C) = -\mathrm{sign}\left(\sin\left(q\pi/p\right)\right). \tag{2.45}$$

This means that up to a power of x

$$\psi(x,t) \approx \exp\left(\eta \widetilde{C} x^{\frac{p+q}{p}}\right) \qquad (\mathrm{Im}\, x = 0,\ \mathrm{Re}\, x \to +\infty) \tag{2.46}$$

with $\widetilde{C}$ real and positive. We expect this semiclassical approximation to be valid everywhere at large $|x|$, except on the cut along the negative x axis. But then the fact that $\psi(x,t)$ is entire means that as we cross the cut, the asymptotic behavior of $\psi(x,t)$ must change from

$$\psi(x,t) \approx \exp\left(\eta \widetilde{C} x^{\frac{p+q}{p}}\right) \qquad (\mathrm{Im}\, x > 0,\ \mathrm{Re}\, x \to -\infty) \tag{2.47}$$

above the negative real axis, to

$$\psi(x,t) \approx \exp\left(\eta \widetilde{C} e^{-2\pi i\left(\frac{p+q}{p}\right)} x^{\frac{p+q}{p}}\right) \qquad (\mathrm{Im}\, x < 0,\ \mathrm{Re}\, x \to -\infty) \tag{2.48}$$

below the negative real axis. Slightly above and below the cut, both contributions (2.47)–(2.48) are present. In order for this to be consistent with the semiclassical approximation, the first contribution must dominate above the cut, while the second must dominate below the cut. Fortunately, this is guaranteed by the sign of $\eta = \mathrm{sign}(C)$ (2.45). It is very satisfying to see how the semiclassical approximation, the level crossing behavior, and the worldsheet calculation of C all fit together so consistently.

Finally, it is worth mentioning that this level crossing behavior is an example of Stokes' phenomenon. We review Stokes' phenomenon in appendix B, and we will discuss its implications for the quantum target space in much greater detail in section 4. [10]

3. An example: the simplest minimal string theory and its FZZT brane

3.1 FZZT correlators and the Kontsevich model

Here we will illustrate the ideas of the previous sections using the example of the $(p,q) = (2,1)$ model, also known as topological gravity. Since this theory is dual to the gaussian matrix model, it allows us to make quite explicit some of the general formulas derived above. Along the way we will encounter a new point of view on the relationship between the Kontsevich matrix model and the double-scaling limit of matrix integrals.

The $(2,1)$ model is represented in the matrix model by the integral

$$\mathcal{Z}(g) = \int dM\ e^{-\frac{1}{g}\mathrm{Tr}\, M^2} \tag{3.1}$$

[10] Another argument that the Baker-Akhiezer function must exhibit Stokes' phenomenon, based on the behavior of eigenvalue distributions, was given in [35, section 3.8]. This argument is related to work of F. David on nonperturbative stability [44] and is also in accord with the discussion of nonperturbative stability at the end of section 5 below.

with M an $N \times N$ hermitean matrix. An FZZT D-brane insertion is represented by the integral

$$\langle \det(x-M) \rangle = \frac{1}{\mathcal{Z}(g)} \int dM \ \det(x-M) e^{-\frac{1}{g}\operatorname{Tr} M^2} . \tag{3.2}$$

Using (2.6), we can write this as an integral over the matrix M and N fermions χ_i. Then we can easily perform the gaussian integral over M in to find the effective theory of the fermions

$$\langle \det(x-M) \rangle = \int d\chi d\chi^\dagger e^{-\frac{g}{4}(\chi^\dagger\chi)^2 + x\chi^\dagger\chi} . \tag{3.3}$$

Note that we started in (3.1) with N^2 degrees of freedom, the entries of M. After gauge fixing they are reduced to the eigenvalues of M, whose number is N. Now we have order N fermions, but their effective theory — which is still invariant under $\mathrm{U}(N)$ — depends only on a single variable $\chi^\dagger\chi$. To make it more explicit we replace (3.3) with

$$\langle \det(x-M) \rangle = \sqrt{\frac{1}{g\pi}} \int ds d\chi d\chi^\dagger \ e^{-\frac{1}{g}s^2 + (is+x)\chi^\dagger\chi} = \sqrt{\frac{1}{g\pi}} \int_{-\infty}^{+\infty} ds \ (x+is)^N e^{-\frac{1}{g}s^2} \tag{3.4}$$

and view s as an effective degree of freedom on the FZZT brane. The final expression as an integral over s is similar to the starting point (3.2). The matrix M is replaced by a single variable s and the determinant is replaced with $(x+is)^N$.

We recognize the r.h.s. of (3.4) as the integral representation of the Hermite polynomials:

$$\langle \det(x-M) \rangle = \left(\frac{g}{4}\right)^{\frac{N}{2}} H_N\left(x\sqrt{\frac{1}{g}}\right) . \tag{3.5}$$

Since these are the orthogonal polynomials of the gaussian matrix model, this confirms explicitly in this example the general result (2.8).

It is trivial to generalize this discussion to n FZZT branes. The partition function of n FZZT branes is given by

$$\langle \det(X \otimes I_N - I_n \otimes M) \rangle = \frac{1}{\mathcal{Z}(g)} \int dM d\chi d\chi^\dagger \ e^{-\frac{1}{g}\operatorname{Tr} M^2 + \chi^\dagger(X\otimes I_N - I_n \otimes M)\chi} \tag{3.6}$$

with X an $n \times n$ matrix and χ_{aj}, $\chi^\dagger_{aj}$ fermions transforming in the bifundamental representation of $\mathrm{U}(n) \times \mathrm{U}(N)$. Integrating out M and integrating back in an $n \times n$ matrix S, we find (after dropping an overall factor)

$$\langle \det(X \otimes I_N - I_n \otimes M) \rangle = \int dS \ \det(X+iS)^N e^{-\frac{1}{g}\operatorname{Tr} S^2} . \tag{3.7}$$

In the large N limit with $g \sim 1/N$, the eigenvalues of M become localized in the interval $(-\sqrt{2}, \sqrt{2})$ along the real axis. The double-scaling limit then corresponds to zooming in on the end of the eigenvalue distribution, while simultaneously bringing the two saddles of (3.4) together. For example, for $n=1$ the double-scaling limit of the FZZT partition function (3.4) is

$$x \to \sqrt{2}\left(1 + \frac{1}{2}\epsilon^2 \hbar^{-2/3} x\right), \quad Ng \to 1 - \epsilon^2\hbar^{-2/3}\tau, \quad s \to \frac{1}{\sqrt{2}}(i - \epsilon s), \quad N \to \epsilon^{-3} \tag{3.8}$$

with $\epsilon \to 0$. Here τ is the lowest-dimension coupling in the continuum theory. Then (3.4) becomes (after dropping overall numerical factors)

$$\psi(x,t) = e^{-x^2/2g}\langle \det(x-M)\rangle \to \int_{-\infty}^{\infty} e^{\frac{1}{3}is^3+i\hbar^{-2/3}(x+\tau)s}\, ds\,. \tag{3.9}$$

We recognize this as the Airy integral; therefore the FZZT partition function is simply

$$\psi(x,t) = Ai\left((x+\tau)\hbar^{-2/3}\right). \tag{3.10}$$

There are a few things to note about this result.

1. The FZZT partition function (3.10) clearly satisfies

$$Q\psi = x\psi\,, \qquad P\psi = \hbar\partial_x\psi \tag{3.11}$$

   with Q and P given by

$$Q = d^2+\tau, \qquad P = Q_+^{1/2} = d\,. \tag{3.12}$$

   (These operators obviously satisfy the string equation $[P,Q] = \hbar$.) This confirms, in this example, that the FZZT partition function is the Baker-Akhiezer function of the KP hierarchy.

2. The Airy function (3.10) is an entire function in the complex x plane. On the real axis, it is oscillatory for $x \le -\tau$ (where classically there is a cut) and decays exponentially for $x > -\tau$. Therefore, although there appear to be two FZZT branes with the same x semiclassically (corresponding to the different sheets of $\mathcal{M}_{2,1}$), we see that the fully nonperturbative FZZT branes depend only on x. The Riemann surface disappears nonperturbatively and is replaced with only its physical sheet.

3. There are, of course, two linearly independent solutions to the equations (3.11). The other solution is the Airy function Bi. We see that it does not correspond to the physical FZZT partition function. Indeed, this solution behaves badly in the semiclassical regime $x \to +\infty$, where it grows exponentially. In terms of (3.9) Bi corresponds to another integration contour.

Now consider the analogous double-scaling limit for the general FZZT correlator (3.7). In this limit, we find

$$e^{-\operatorname{Tr}X^2/2g}\langle \det(X\otimes I_N - I_n\otimes M)\rangle \to \int dS\; e^{\operatorname{Tr}\left(iS^3/3+i\hbar^{-2/3}(X+\tau)S\right)} \tag{3.13}$$

which is, of course, the $n\times n$ Kontsevich model (for a review of the Kontsevich model and topological gravity, see e.g. [42]). Through the use of the fermions, we have obtained a rather direct route from the gaussian matrix model to the Kontsevich model. We also see quite explicitly how the matrix S of the Kontsevich model is the effective degree of freedom describing open strings stretched between n FZZT branes, an insight obtained in [24].

Note that we can also think of the FZZT correlator (3.13) as a perturbation around the closed-string background corresponding to $(p,q) = (2,1)$. This is a trivial statement at finite N: it simply means that the insertion of determinants at positions $x_1, \ldots, x_n$ is equivalent to a certain shift in the matrix model potential. This shift can be obtained by writing $\det(x_i - M)$ as $e^{\mathrm{Tr}\log(x_i - M)}$ and expanding the logarithm at large x_i. In the continuum limit, essentially the same story holds, except that now we must expand $\log(x - M)$ in the basis of scaling potentials $W_k(M)$ for a single cut model. For a cut between $-\sqrt{2}$ and $\sqrt{2}$, these potentials take the form [6]

$$W_k'(M) = (2k+1)2^{(k-1)/2}\left[(M-\sqrt{2})^k\left(1+\frac{2\sqrt{2}}{M-\sqrt{2}}\right)^{1/2}\right]_+ , \tag{3.14}$$

where $[\,]_+$ indicates that we expand in powers of $1/M$ and keep only positive powers of M. Thus as $N \to \infty$, each determinant insertion $\det(x - M)$ can be viewed as a modification of the potential

$$\mathrm{Tr}\ V'(M) \to \mathrm{Tr}\ V'(M) + \sum_{k=0}^{\infty} t_{2k+1}\,\mathrm{Tr}\ W_k'(M)\,, \tag{3.15}$$

where the couplings are given by

$$t_{2k+1} = \frac{2^{-(k-1)/2}}{2k+1}(x-\sqrt{2})^{-k-1}\left(1+\frac{2\sqrt{2}}{x-\sqrt{2}}\right)^{-1/2} . \tag{3.16}$$

This formula for t_{2k+1} can be verified by, e.g. writing the scaling potentials (3.14) as contour integrals around infinity and then performing the sum (3.15) explicitly.

In the double scaling limit we zoom in on $x \sim \sqrt{2}$ as in (3.9) (we set $\hbar = 1$ and $\tau = 0$ for simplicity). Summing over $i = 1, \ldots, n$, we find that the t_k's reduce to

$$t_{2k+1} = \frac{1}{2k+1}\sum_{i=1}^{n} x_i^{-k-1/2} . \tag{3.17}$$

Therefore the $(2,1)$ model with n FZZT branes can be thought of as the closed-string background with the couplings (3.17) turned on.

To identify properly the precise value of the closed-string partition function, we must also take into account the fact that $\mathcal{Z}_{\mathrm{closed}}(t) \to 1$ as $t \to 0$ (which is the same as $x_i \to \infty$). In this limit, with $x_i \to +\infty$, the double-scaled FZZT correlator reduces to the WKB approximation of the matrix Airy integral (3.13). Thus we must divide by this quantity to extract the closed-string partition function. In other words, we have shown that in the double-scaling limit,

$$e^{-\mathrm{Tr}\,X^2/2g}\langle \det(X\otimes I_N - I_n \otimes M)\rangle \to C(X)\mathcal{Z}_{\mathrm{closed}}(t) \tag{3.18}$$

with

$$C(X) = e^{-2\,\mathrm{Tr}\,X^{3/2}/3}\int dS\ e^{-\mathrm{Tr}\,\sqrt{X}S^2} . \tag{3.19}$$

Equating (3.13) and (3.18), (and setting $\hbar = 1, \tau = 0$) we arrive at the relation

$$\mathcal{Z}_{\text{closed}}(t) = \frac{\int dS\ e^{\mathrm{Tr}\left(iS^3/3 + iXS + 2X^{3/2}/3\right)}}{\int dS\ e^{-\mathrm{Tr}\sqrt{X}S^2}}\,. \tag{3.20}$$

Note that by shifting the S integral in the numerator, we can rewrite this as

$$\mathcal{Z}_{\text{closed}}(t) = \frac{\int dS\ e^{\mathrm{Tr}\left(iS^3/3 - ZS^2\right)}}{\int dS\ e^{-\mathrm{Tr}\,ZS^2}} \tag{3.21}$$

with

$$Z = \sqrt{X}\,. \tag{3.22}$$

Equation (3.21) is the way the relation between the finite n Kontsevich model and topological gravity is usually stated. Here we have rederived this fact directly from double-scaling gaussian matrix model.

There are a few interesting things to note in our derivation. First, the normalizing factor $C(X)$, being the WKB approximation to the (matrix) Airy function, is not an entire function of the eigenvalues of X. For instance, it has the simple form $(2\sqrt{\pi}x)^{-1/4}e^{-2x^{3/2}/3}$ when $n = 1$, and this clearly has branch cuts in the complex x plane.[11] This explains why the usual relation (3.21) between the closed-string partition function and the Kontsevich integral suffers from branch cuts as a function of (the eigenvalues of) X. On the other hand, we see that the combination $C(X)\mathcal{Z}_{\text{closed}}(t)$, being the matrix Airy integral, is an entire function of X, even though the separate factors are not.

The second point worth mentioning is the interpretation of the quantity $Z = \sqrt{X}$ (or $Z = \sqrt{X + \tau}$ for nonzero cosmological constant) that emerged naturally in our derivation. This quantity also featured in the work of [24], where it corresponded to the boundary cosmological constants of n FZZT branes. In order to compare with the results of [24], one needs to keep in mind that in [24] the Liouville coupling constant was taken to be $b^2 = 1/2$, while here we are assuming $b^2 = 2$. Thus, their boundary cosmological constant is equal to our dual boundary cosmological constant $\widetilde{\mu}_B = \sqrt{\mu_B + \tau} = \mu_B|_{there}$. With our definitions, the FZZT brane labelled by μ_B is the one corresponding to $\det(\mu_B - M)$ in the double-scaled gaussian matrix model. This corresponds to treating the worldsheet boundary interaction $\mu_B e^{b\phi}$ as a non-normalizable operator. From the point of view of Liouville theory with $b^2 = 2$ it is more natural to consider FZZT branes as a function of $\widetilde{\mu}_B$, which corresponds to treating the worldsheet boundary interaction $\widetilde{\mu}_B e^{\frac{1}{b}\phi}$ as a non-normalizable operator. The expectation values of the FZZT branes with these two choices are related, at the classical level, by a Legendre transform. When we quantize open strings on the FZZT brane it looks like we have a choice of which operator to fix. These two choices amount to different quantization prescriptions for the open strings, analogous to the different choices in other AdS/CFT examples [45]. It seems that the open string field theory of [24] corresponds to considering fluctuations of $\widetilde{\mu}_B$. This ends up performing a Fourier transform between the result for fixed $\widetilde{\mu}_B$, which is a simple exponential, and the result at fixed μ_B, which is given by the Airy integral.

[11] Note that this is consistent with the asymptotic expansion at large x of our general result (2.20).

3.2 The quantum resolvent in the gaussian matrix model

The gaussian matrix model also provides a good setting for the discussion of the quantum resolvent in section 2.4. Substituting (3.10) into (2.26), we find the quantum eigenvalue density

$$\rho_\hbar(\lambda) = \hbar^{1/3} Ai'((\lambda+\tau)\hbar^{-2/3})^2 - \hbar^{-1/3}(\lambda+\tau)Ai((\lambda+\tau)\hbar^{-2/3})^2 \tag{3.23}$$

One can check that this is everywhere positive on the real axis. Using the asymptotic expansions

$$Ai(x) \sim \begin{cases} \dfrac{1}{2\sqrt{\pi}x^{1/4}} e^{-2/3x^{3/2}} & |\arg(x)| < \pi \\ \dfrac{1}{\sqrt{\pi}(-x)^{1/4}} \sin\left(\dfrac{\pi}{4} + \dfrac{2}{3}(-x)^{3/2}\right) & \arg(x) = \pi \end{cases} \tag{3.24}$$

we see that the classical limit of the eigenvalue density on the real axis is as expected:

$$\lim_{\hbar\to 0} \rho_\hbar(\lambda) = \begin{cases} \dfrac{\hbar}{8\pi(\lambda+\tau)} e^{-\frac{4}{3\hbar}(\lambda+\tau)^{3/2}} & \lambda > -\tau \\ \dfrac{\sqrt{-(\lambda+\tau)}}{\pi} & \lambda < -\tau \end{cases} . \tag{3.25}$$

Now consider the quantum resolvent. Since $\rho_\hbar$ is positive on the real axis, the quantum resolvent (2.25) is indeed discontinuous across the entire real axis. Combining (2.30) with (3.24), we see that the resolvents R_+ and R_- only differ by a small, nonperturbative amount in a wedge around the positive real axis (we now set $\tau = 0$ for simplicity).

$$R_+(x) - R_-(x) \sim \frac{i\hbar}{4x} e^{-\frac{4}{3\hbar}x^{3/2}}, \qquad |\arg(x)| \leq \frac{\pi}{3} . \tag{3.26}$$

Let us call this wedge region I. By the same argument, the resolvents differ by a *large* amount in the wedge $\frac{\pi}{3} < |\arg(x)| \leq \pi$, which we will call region II. In other words, the small nonperturbative quantity (3.26) in region I becomes a large nonperturbative quantity in region II. In region II, the resolvent R_+ has the correct classical limit in the upper half plane, while the resolvent R_- has the correct classical limit in the lower half plane.

To find the second sheet of the Riemann surface, we must first take the classical limit of R_+ (R_-) in the union of region I and the upper (lower) half plane. Only by dropping the nonperturbative corrections does the branch cut at $x < 0$ appear. Then we can analytically continue through this cut to find the second sheet.

4. The effective theory on the brane

We have seen in the previous two sections how the Riemann surface disappears nonperturbatively, with the FZZT partition function being an entire function of the complex x plane. Here we would like to understand this nonperturbative modification in more detail, from the point of view of the effective theory on the FZZT brane. We will limit ourselves to the simplest case of $(2,1)$, in which case the effective theory (3.13) on n FZZT branes is the $n \times n$ Kontsevich model [24]. For simplicity, we will consider only the case $n = 1$.

The semiclassical approximation of $\hbar \to 0$ corresponds to the saddle-point approximation. For the FZZT partition function (3.9), there are two saddle points in the s integral, located at

$$\langle s \rangle = \pm \hbar^{-1/3} \sqrt{-x}\,. \tag{4.1}$$

(For simplicity we set $\tau = 0$.) Therefore, there are two distinct branes for each x, semiclassically. The moduli space of branes becomes a double cover of the x plane, as we saw in the introduction.

Contrast this now with the quantum theory. Here we must integrate over s; i.e. we must study the quantum dynamics of the theory on the brane. The subleading saddles in the integral over s are *instantons* in the theory on the brane. As is always the case with instantons, one must sum over them in some prescribed fashion. The result of this process is that the exact, nonperturbative FZZT partition function becomes an entire function of x. For $(2,1)$ it is the Airy function (3.10).

The crucial point is that instead of exhibiting monodromy around $x = \infty$, the FZZT partition function now exhibits what is known as Stokes' phenomenon. As we discussed in the introduction, this is the phenomenon whereby the analytic continuation of the asymptotics of a function in one region does not correctly reproduce the asymptotics of the function in another region. (See also appendix B for a brief review of Stokes' phenomenon, summarizing [39].)

The Airy function is actually a paradigmatic example of Stokes' phenomenon. In the region $x \to +\infty$, the Airy function is given approximately by

$$Ai(x) \sim \frac{1}{2\sqrt{\pi} x^{1/4}} e^{-\frac{2}{3}x^{3/2}}\,. \tag{4.2}$$

Attempting to analytically continue the asymptotics counterclockwise around large x to $x \to -\infty$, one would find $Ai(x) \sim e^{+\frac{2}{3}i(-x)^{3/2}}$ there. However, the correct asymptotics of the Airy function on the negative real axis is actually

$$Ai(x) \sim \frac{1}{\sqrt{\pi}(-x)^{1/4}} \sin\left(\frac{\pi}{4} + \frac{2}{3}(-x)^{3/2}\right) \tag{4.3}$$

i.e. it is a linear combination of the two saddles (4.1).

The reason this happened is that as we varied x from $x = +\infty$ to $x = -\infty$, we crossed a Stokes' line at

$$\arg(x) = \pm \frac{2\pi}{3}\,. \tag{4.4}$$

Recall from the introduction that Stokes' lines are the places where various saddle-point contributions to an integral appear and disappear. In our example, one can see this by starting from the negative real axis, where according to (4.3), both saddles contribute to the Airy integral. Upon crossing the Stokes' lines (4.4), however, the subdominant saddle disappears entirely from the asymptotic expansion, until one reaches the positive real axis, where the function is given by (4.2). The Stokes' lines occur at precisely the points where the disappearing saddle is most subdominant.

We can also describe the effect of Stokes' lines in a slightly different way: the presence of Stokes' lines implies that in some regions, certain saddle points might not contribute at all to the integral. Therefore, the naive procedure of just summing over all the saddle points is not valid here. A case in point is again the $x \to +\infty$ asymptotics of the Airy function (4.2). There we see that the function is dominated by just one saddle. The other saddle clearly does not contribute; if it did, it would contribute an exponentially *increasing* contribution to the Airy function at $x \to +\infty$.

Let us conclude this section by briefly summarizing two general lessons we can learn from this example.

1. The classical saddle-point approximation is certainly valid, but in the exact quantum answer, we might need to sum over saddles. Because of Stokes' phenomenon, not all the saddles necessarily contribute in various asymptotic regions. Even the dominant saddle sometimes does not contribute.[12]

2. The quantum target space (the complex x plane) differs significantly from the classical target space (the Riemann surface). The various unphysical sheets of the Riemann surface disappear, also because of Stokes' phenomenon. In a wedge around the erstwhile branch cut, what were classically interpreted as the unphysical sheets lead to exponentially small corrections to the exact, quantum answer.

5. Comments on other backgrounds

In section 2, we extracted the asymptotics of the FZZT partition function $\psi(x,t)$ at large positive x and small $\hbar$ for general (p,q). Combining this with the fact that $\psi(x,t)$ is an entire function of x, we argued that $\psi(x,t)$ exhibited Stokes' phenomenon. Thus, we expect that our conclusion above about the disappearance of the Riemann surface is generally true and that this phenomenon comes about in a way similar to what we saw in the $(p = 2, q = 1)$ model. Certain regions in the unphysical sheets lead to small nonperturbative corrections to the semiclassical answer in the physical sheet. Meanwhile, other regions in the unphysical sheets do not contribute such effects.

However, a true generalization of our analysis from $(2,1)$ to other values of (p,q) requires clarification of two issues: first, the role of the ZZ branes, which exist for higher (p,q) but not for $(2,1)$, and second, the overall nonperturbative consistency of models with higher (p,q).

First, let us discuss the ZZ branes. Recall that at the classical level, the number of background ZZ branes is measured by the A-periods of the one-form ydx on the Riemann surface $\mathcal{M}_{p,q}$ [23]:

$$\oint_{A_i} ydx = N_i \hbar\,, \tag{5.1}$$

where N_i is the number of ZZ branes of type i. In the simplest backgrounds without ZZ branes the A-periods vanish and the surface degenerates to a genus zero surface. The moduli of $\mathcal{M}_{p,q}$ fall into two classes [23, 26]. Moduli which preserve the A-periods correspond to closed string backgrounds. Moduli which change the values of these periods arise only when ZZ branes are added.

[12] The relation between the various sheets of the Riemann surface and the exact answer was explored also in [46] , where the proposal seems to be to sum over all saddles.

It is clear that this picture must be modified in the exact quantum theory. Even without a nonperturbative definition of the theory it is clear that the periods $\oint_{a_i} ydx = N_i\hbar$ are quantized when $\hbar \neq 0$ and therefore they cannot change in a continuous fashion by varying moduli. But in order to understand the exact nonperturbative theory, we need a definition of the theory which goes beyond the worldsheet expansion. We take the double scaled matrix model to be this definition.

In the matrix model, the ZZ branes represent eigenvalue instantons, corresponding to sub-leading saddles of the matrix integral where some of the eigenvalues are away from the cut. Thus, unlike the classical theory, which is characterized by fixed values of the integers N_i, in the exact theory we must sum over the N_i. This sum over ZZ branes is automatically incorporated in the exact, nonperturbative matrix integral. In the end, the exact answer is characterized only by the closed string backgrounds.

The second issue concerns the nonperturbative existence of the (p, q) models. It is well known that certain values of (p, q) (e.g. $(p, q) = (2, 3)$, corresponding to pure gravity) do not exist nonperturbatively [44]–[49] and[35, 36]. This happens when the double-scaled matrix model potential is not bounded from below. We can study this problem in the continuum using the FZZT partition function and its relation to the effective potential [22, 23, 26]

$$\psi(x,t) \approx e^{-V_{eff}(x)/2\hbar}\,. \tag{5.2}$$

For large $|x|$ away from the negative real axis we have from (2.46)

$$\frac{1}{2\hbar}V_{\rm eff}(x) \approx -\eta\widetilde{C}x^{\frac{q+p}{p}}\,. \tag{5.3}$$

Therefore, the effective potential is bounded from below only when [26]

$$\eta = -\text{sign}\left(\sin\left(\frac{q\pi}{p}\right)\right) < 0\,. \tag{5.4}$$

For example, in the $(p = 2, q = 2l - 1)$ models (5.4) is satisfied only for l odd, and it is never true in the unitary models with $(p, q = p + 1)$.

Notice that for the nonperturbatively consistent models, $\psi(x, t)$ vanishes as $x \to +\infty$. This reflects the fact that the eigenvalues are not likely to be found there. This also specifies boundary conditions for the differential equations (2.14) satisfied by ψ, and these boundary conditions are sufficient to determine uniquely $\psi(x, t)$. Conversely, in the nonperturbatively inconsistent models the semiclassical value of $\psi(x, t)$ diverges as $x \to +\infty$. Thus there is a nonperturbative ambiguity in the definition of $\psi(x, t)$ corresponding to the freedom to add small exponential corrections to the dominant contribution (5.2). So we see how the nonperturbative problems of these models, which are associated with the unboundedness of the potential, manifest themselves here in the ambiguity of defining the FZZT partition function $\psi(x, t)$.

6. Summary and discussion

We have explored the relation between the semiclassical geometry seen by the FZZT branes in minimal string theory and the exact results as computed by the matrix model. We have seen that the various sheets of the Riemann surface correspond to different saddle

JHEP10(2004)020

points of the effective theory on the FZZT brane. For some ranges of the value of the boundary cosmological constant all the saddles contribute to the answer, while for some other ranges only a subset of all saddles contribute. The precise matrix model definition of the theory tells us which saddles contribute and which do not contribute. So the Riemann surface, which plays a crucial role in the perturbative analysis of the model, suffers drastic modifications when we consider the full nonperturbative aspects of the theory.

We have also given a quick derivation of the relation between the Kontsevich matrix model and the ordinary double scaled matrix model, clarifying the relation between the various open string descriptions of the theory. The Kontsevich model arises as the effective theory on the FZZT branes [24] after integrating out all the open strings corresponding to the ZZ branes. The degrees of freedom of the Konsevich model are, roughly speaking, "mesons" made out of the fermionic strings stretched between FZZT and ZZ branes [26].

We have discussed in detail the simplest $(2,1)$ model, but we also argued on general grounds that the disappearance of the Riemann surface due to Stokes' phenomenon is a feature of all of the (p,q) models.

Our paper was partially motivated by the discussion of physics behind the horizon in [37] . We have a somewhat similar problem. The Riemann surface is analogous to spacetime and the second sheet is analogous to the region behind the horizon. The FZZT brane observables could be viewed as probes of the spacetime geometry. Note that the parameter $x = \mu_B$ is controlled in the boundary region "outside" the horizon. By analytically continuing semiclassical answers we get to explore the second sheet of the Riemann surface, much in the same way that the region behind the horizon is explored in [37] . The black hole singularity, where quantities diverge, is somewhat analogous to the $x \to \infty$ region of the second sheet, where again the expectation values of the analytically continued FZZT branes diverge. In the exact answer, however, this saddle point ceases to contribute before its value becomes very large. In both cases, the holographic theory tells us that there are no divergences in this region. We expect that further analysis of these simple exactly solvable examples might yield interesting general lessons for how to think about quantum gravity in higher dimensions.

Another motivation for our work was the resemblance, at least at the perturbative level, between the minimal string theories and the topological string (see, e.g. the discussion of the $(p,1)$ models in [38]). Nonperturbatively, however, the connection is less clear. While we lack a generally accepted nonperturbative definition for the topological string, minimal string theories have an exact, nonperturbative formulation in terms of the dual matrix model. Given the similarities between the two theories, it is natural to suppose that some of the lessons from our work might be relevant to the topological string. Let us just briefly mention a few.

First, we have seen how the semiclassical target space (the Riemann surface) is drastically modified by nonperturbative effects. In the topological string, the Riemann surface is intimately connected with the target space. The Riemann surface is the surface $H(x,y) = 0$ in $\mathbb{C}^2$. The Calabi-Yau is given by the equation $uv + H(x,y) = 0$ in $\mathbb{C}^4$. This Calabi-Yau is a $\mathbb{C}$-fibration over the complex (x,y) plane, and the discriminant locus of the fibration is the Riemann surface $H(x, y) = 0$. Our results raise the question of whether in a proper nonperturbative definition of the topological string the Calabi-Yau might also be drastically modified by quantum effects.

Another striking feature of our analysis is the role of Stokes' phenomenon. Semiclassical target space is viewed as a saddle-point approximation to some effective theory on the brane probe. Nonperturbatively, we must sum over different saddle-points in a prescribed fashion. As we saw with the Airy function, the result was that some portions of the semiclassical target space contributed to physical observables, while others did not. It even happened sometimes that the dominant saddle-point did not contribute. It will be interesting to see if these phenomena play a role in the nonperturbative topological string.

A third possible application to the topological string is the role of the ZZ branes. These correspond to eigenvalue instantons in the matrix model. The classical vacuum of the matrix model corresponds to placing all of the eigenvalues into the dominant minimum of the matrix model potential. However, in the exact answer we must sum over all vacua (i.e. sum over all instantons), obtained by filling the other critical points of the potential with any number of eigenvalues. In the continuum limit, this means that we must integrate over a subset of the moduli of the Riemann surface describing the normalizable deformations due to ZZ branes. Note that the closed-string couplings are non-normalizable deformations, and hence we do not integrate over them. This suggests that in the nonperturbative topological string, one should also integrate over some of the moduli of the Calabi-Yau (the normalizable modes) but not others.

In the context of the topological string, it has been suggested that the Riemann surface is covered by patches and the D-branes in different patches are related by (generalized) Fourier transform [38, 46]. Comparison with the two matrix model suggests, as mentioned in footnote 3, that the theory has two distinct branes $\det(x - M)$ and $\det(y - \widetilde{M})$. As in [40], these are natural in different patches on $\mathcal{M}_{p,q}$ consisting of the first sheet of the x-plane and the first sheet of the y-plane (note that these two patches do not generally cover the whole surface). As in [23, 40], in the classical theory these branes are related by Legendre transform, with the boundary cosmological constant x and its dual y satisfying the defining equation of $\mathcal{M}_{p,q}$. It is likely that nonperturbatively they are related by a Fourier transform. This can be interpreted as a relation between different branes rather than as a relation between different patches of the surface.

Finally, let us mention a more mathematical potential application of our work. We have seen that the asymptotics of the Baker-Akhiezer function (2.31) shows very clearly the emergence of the classical Riemann surface through the one-form ydx. It is an old idea [36] that the full Baker-Akhiezer function should be used to define a "quantum Riemann surface," associated with the string equations $[P, Q] = \hbar$ in a way analogous to the association of a Riemann surface to the stationary KdV equations, in which case $[P, Q] = 0$. A closely related point is the relation of the matrix model partition function and KdV flows to the infinite grassmannian. In particular, in the free fermion interpretation of the infinite grassmannian one needs to introduce an operator which does not create monodromy, (such as twistfields in conformal field theory) but rather Stokes multipliers. Such operators, called "star operators" in [35, 36], are not at all well-understood. It was suggested in [35, 36] that the point in the grassmannian created by star operators should define a "theory of free fermions on a quantum Riemann surface." A similar suggestion has recently been made in [38]. Perhaps it is a good time to revisit these issues.

Acknowledgments

We would like to thank S. Shenker for useful discussions. G.M. would like to thank the Aspen Center for Physics for hospitality during the completion of this paper. The research of J.M. and N.S. is supported in part by DOE grant DE-FG02-90ER40542. The research of GM is supported in part by DOE grant DE-FG02-96ER40949. The research of D.S. is supported in part by an NSF Graduate Research Fellowship and by NSF grant PHY-0243680. Any opinions, findings, and conclusions or recommendations expressed in this material are those of the author(s) and do not necessarily reflect the views of the National Science Foundation.

A. Geometric interpretation of the Lax formalism

In this appendix, we will study the Lax operators Q and P in the semiclassical $\hbar \to 0$ limit. Much of this section will consist of collecting and streamlining many facts that are scattered throughout the literature. However, in the process of organizing this material, several new insights will emerge.

Our main goal is to provide a geometric interpretation for P and Q in terms of the Riemann surface $\mathcal{M}_{p,q}$ of minimal string theory. How this geometric interpretation is modified at $\hbar \neq 0$ is an important question. In [36], it was proposed that by generalizing the Burchnall-Chaundy-Krichever theory of KdV flow, phrased in terms of framings of line bundles, to framings of a flat holomorphic vector bundle over the space of x, t_j, one could define a notion of a "quantum Riemann surface." It would be nice to understand the relation of this proposal to the geometrical interpretation given below.

A.1 A brief review of the Lax formalism

First, let us take a moment to recall briefly the definition of the Lax operators Q and P of minimal string theory. (For a more thorough review, see e.g. [10].) These operators are a convenient way to package neatly the data (physical correlation functions) of minimal string theory. They are differential operators, of degree p and q respectively, in

$$d = \hbar \partial_\tau \,, \tag{A.1}$$

where $\tau = t_1$ is the coupling to the lowest-dimension operator. Explicitly, we have

$$\begin{aligned} Q &\propto d^p + \frac{1}{2}\sum_{j=2}^{p} \{u_{p-j}(t), d^{p-j}\} \\ P &\propto d^q + \frac{1}{2}\sum_{j=2}^{q} \{v_{q-j}(t), d^{q-j}\} \,, \end{aligned} \tag{A.2}$$

where the coefficients $u_{p-j}(t)$ and $v_{q-j}(t)$ represent various two-point functions of physical closed-string operators. They depend on the closed-string couplings $t = (t_1, t_2, \ldots)$. For instance,

$$u_{p-2}(t) \propto \partial_\tau^2 \log \mathcal{Z} \tag{A.3}$$

corresponds to the “specific heat” of the string theory.

To solve minimal (closed) string theory, we simply need to solve for the dependence of Q and P on the closed-string couplings $t = (t_1, t_2, \ldots)$. This is done by requiring that Q and P satisfy the string equation

$$[P, Q] = \hbar \tag{A.4}$$

along with the KdV flows

$$\hbar \frac{\partial Q}{\partial t_j} = [Q, Q_+^{j/p}] , \qquad \hbar \frac{\partial P}{\partial t_j} = [P, Q_+^{j/p}] . \tag{A.5}$$

The compatibility of the latter with the former implies that P is given in terms of Q by

$$P = \sum_{\substack{k \geq 1 \\ k \neq 0 \bmod p}} (1 + k/p)\; t_{k+p}\; Q_+^{k/p} . \tag{A.6}$$

Substituting this back into (A.4) then gives a set of coupled differential equations for the coefficient functions of Q. These equations can be solved order by order in $\hbar$, resulting in a perturbative expansion for P and Q

$$\begin{aligned} Q &= Q_0(d,t) + \hbar\, Q_1(d,t) + \hbar^2\, Q_2(d,t) + \cdots \\ P &= P_0(d,t) + \hbar\, P_1(d,t) + \hbar^2\, P_2(d,t) + \cdots , \end{aligned} \tag{A.7}$$

where by convention the operators on the r.h.s. of (A.7) are ordered such that the d's are all on the right.

A.2 The Lax operators in the semiclassical limit

Now let us take $\hbar \to 0$ to obtain a much simpler set of equations for the Lax operators. In this limit, the string equation (A.4) becomes

$$\frac{\partial P_0}{\partial d} \frac{\partial Q_0}{\partial \tau} - \frac{\partial P_0}{\partial \tau} \frac{\partial Q_0}{\partial d} = 1 \tag{A.8}$$

i.e. the commutator is replaced with a Poisson bracket. To see this, note that every time $d = \hbar \partial_\tau$ acts on something to its right, it contributes a factor of $\hbar$. Therefore the leading order contribution to the commutator is the Poisson bracket (A.8).

The solution to this equation is well-known (see e.g. [10, section4.5]). It is simply

$$P_0(d; t) = y(x; t) \qquad \text{with } x = Q_0(d; t) , \tag{A.9}$$

where $y(x; t)$ is the singular part of the large N matrix model resolvent in the closed-string background labelled by t. Since (x, y) lie on the Riemann surface $\mathcal{M}_{p,q}$, (A.9) implies that at $\hbar = 0$, the simultaneous eigenvalues of Q_0 and P_0 also lie on the same Riemann surface, i.e.

$$(Q_0, P_0) \in \mathcal{M}_{p,q}\,. \tag{A.10}$$

The fact that they can be written in the form (A.2) as polynomials in d implies that the eigenvalue of d is the uniformizing parameter for $\mathcal{M}_{p,q}$. Thus we can write (A.9) as follows:

$$Q_0 = x(z = d; t)\,, \qquad P_0 = y(z = d; t)\,. \tag{A.11}$$

Thus we have reduced the algebraic-differential problem of solving the genus zero string equation to the geometric problem of finding the uniformizing parameter of $\mathcal{M}_{p,q}$. This problem has been solved in various special cases. For instance, in [23], it was found that

$$x(z) = T_p(z)\,, \qquad y(z) = T_q(z) \tag{A.12}$$

in the conformal background. (To keep the equations simple in this appendix, we will rescale y so as to remove the coefficient C. This will have no effect on arguments below.)

Although it is in general a nontrivial exercise to extract from the string equation the higher order $\hbar$ corrections to the Lax operators, it is actually easy to obtain the first order $\hbar$ corrections Q_1 and P_1. This is because the coefficient functions of Q and P, being closed-string observables, have an expansion in $\hbar^2$ (the closed-string coupling), not $\hbar$ (the open string coupling). (Note that this statement is only true for the particular ordering prescription we used in defining the Lax operators (A.2).) Thus Q_1 and P_1 arise only from the non-commutation of d and the coefficient functions. This gives

$$Q_1 = \frac{1}{2}\partial_\tau \partial_z x(z,\tau)|_{z=d}\,, \qquad P_1 = \frac{1}{2}\partial_\tau \partial_z y(z,\tau)|_{z=d}\,. \tag{A.13}$$

Here we have used (A.11), and, as noted above, Q_1 and P_1 are defined with the d's all on the right.

Finally, we should note that the discussion of P and Q in this appendix is limited to the classical backgrounds without ZZ branes, where the surface $\mathcal{M}_{p,q}$ has genus zero and a number of pinched cycles. It will be interesting to see how to generalize this discussion to backgrounds with ZZ branes present. Then the pinched cycles of $\mathcal{M}_{p,q}$ are opened up and the surface no longer has genus zero. In such backgrounds, z is no longer a good uniformizing parameter, and our interpretation of P and Q will have to be modified accordingly.

KdV flow and deformations of $\mathcal{M}_{p,q}$. Having shown that the simultaneous eigenvalues of Q and P (we will drop the subscript 0 from this point onwards) are nothing but the coordinates (x, y) of $\mathcal{M}_{p,q}$, we can now provide a geometric interpretation of the KdV flow equations (A.5). The KdV flows tell us how to deform Q and P from a closed-string background t to a nearby background $t + \delta t$. This gives rise to a deformation of $\mathcal{M}_{p,q}$. Therefore, on general grounds, the genus-zero KdV flows must be equivalent to the singularity-preserving deformations of $\mathcal{M}_{p,q}$ discussed in [23].

We can check our claim explicitly in the conformal background. After a lengthy calculation, whose details we will skip, one derives the following deformations of P and Q from the KdV flow equations (A.5):

$$\frac{\partial Q}{\partial \tau_{r,s}} = \frac{1}{q} U_{p-1}(d) \left[\frac{T_{ps}(d) U_{qr-1}(d)}{U_{p-1}(d) U_{q-1}(d)}\right]_- \tag{A.14}$$

and

$$\frac{\partial P}{\partial \tau_{r,s}} = \frac{1}{p}U_{q-1}(d)\left[\frac{T_{qr}(d)U_{ps-1}(d)}{U_{p-1}(d)U_{q-1}(d)}\right]_{-} - \frac{1}{p}U_{q-1}(d)\left[\frac{U_{qr-ps-1}(d)}{U_{q-1}(d)U_{p-1}(d)}\right]_{+} \tag{A.15}$$

in the conformal background, up to an overall normalization factor. Here $\tau_{r,s}$ is the coupling associated to the continuum operator $\mathcal{V}_{r,s}$; it is related to the matrix model couplings t_j by a linear transformation. (The change of basis between matrix model and continuum couplings is discussed in [29].) It is important that both (A.14) and (A.15) are polynomials in d; this is required by the definition of Q and P. Note also that the degree of the deformation to Q is always less than p, but there is no restriction on the degree of the deformation to P.

Since the curve for $\mathcal{M}_{p,q}$ in the conformal background is

$$F(Q,P) = T_q(Q) - T_p(P) = 0 \tag{A.16}$$

the deformation to the curve due to (A.14)–(A.15) is

$$\begin{aligned}\frac{\partial F}{\partial \tau_{r,s}} &= U_{q-1}(Q)U_{p-1}(d)\left[\frac{T_{ps}(d)U_{qr-1}(d)}{U_{p-1}(d)U_{q-1}(d)}\right]_{-} - U_{p-1}(P)U_{q-1}(d)\left[\frac{T_{qr}(d)U_{ps-1}(d)}{U_{p-1}(d)U_{q-1}(d)}\right]_{-} + \\ &\quad + U_{p-1}(P)U_{q-1}(d)\left[\frac{U_{qr-ps-1}(d)}{U_{q-1}(d)U_{p-1}(d)}\right]_{+} \\ &= U_{pq-1}(d)\left(\frac{T_{ps}(d)U_{qr-1}(d) - T_{qr}(d)U_{ps-1}(d)}{U_{p-1}(d)U_{q-1}(d)}\right).\end{aligned} \tag{A.17}$$

In the second line, we have substituted (A.12) for Q and P and we have used the identity $U_{m-1}(T_n(z)) = U_{mn-1}(z)/U_{n-1}(z)$. Further use of this identity leads to

$$\frac{\partial F}{\partial \tau_{r,s}} = U_{q-1}(Q)T_s(Q)U_{r-1}(P) - U_{p-1}(P)T_r(P)U_{s-1}(Q) \tag{A.18}$$

which agrees exactly with the singularity-preserving deformations of $\mathcal{M}_{p,q}$ found in [23]. This confirms very explicitly the equivalence between the KdV flows and the deformations of $\mathcal{M}_{p,q}$.

We should mention that for $p=2$, the equivalence of the KdV flows and the singularity-preserving deformations of $\mathcal{M}_{p,q}$ can be seen more directly using the formulas in [35, 36]. There it is shown, using the representation of the KdV equations as first-order matrix equations, that one can define an "$\hbar$-deformed" Riemann surface $y^2 = F(x;t,\hbar)$ which reduces as $\hbar \to 0$ to the classical Riemann surface (what we call $\mathcal{M}_{p,q}$) of the matrix model. Here $F(x;t,\hbar)$ is a polynomial in x, which depends in a complicated way on the closed string couplings t. Although we will not discuss the details here, one can show that at $\hbar = 0$, the Riemann surface reduces to

$$y^2 = (x + u(t))\,(B(x;t))^2\ , \tag{A.19}$$

where $B(x,t)$ is a polynomial in x as well as in the Gelfand-Dickii potentials $R_j[u]$. (See [35, eq. (2.35)].) The form (A.19) shows immediately that the KdV flows are singularity-preserving deformations of $\mathcal{M}_{p,q}$, since as we change the couplings t, the r.h.s. of (A.19) always has only one branch point at $x = -u(t)$ and singularities at the roots of $B(x;t)$.

It is interesting to contrast this with the Burchnall-Chaundy-Krichever theory of stationary KdV flows. There the Riemann surface is obtained from simultaneous eigenvalues of the differential operators $[P,Q] = 0$. The KdV flow preserves the Riemann surface moduli and instead is straight-line flow along the jacobian of the Riemann surface [50].

Instantons and the singularities of $\mathcal{M}_{p,q}$. Finally, we will discuss the connection between instantons and the singularities of $\mathcal{M}_{p,q}$. Instantons were studied using the classical limit of the Lax formalism by Eynard and Zinn-Justin in [51]. Let us briefly review the logic of their analysis. To leading order, an instanton corresponds to an exponentially-suppressed perturbation $\epsilon(t)$ of the specific heat $u(t)$ and all other physical correlation functions. Thus in the $\hbar \to 0$ limit, we can write

$$\frac{\epsilon'}{\epsilon} = r\sqrt{u(t)} \tag{A.20}$$

for some constant r which measures the strength of the instanton. (The derivative in (A.20) is with respect to the lowest-dimension coupling τ.) Since as $\hbar \to 0$ we can ignore the t dependence of $u(t)$, we might as well set $u(t) = 1$. Then (A.20) can be written as $d\epsilon = \epsilon(d+r)$, which implies that

$$f(d)\epsilon = \epsilon f(d+r) \tag{A.21}$$

for any function $f(d)$.

The next step in the analysis of [51] is the observation that the instanton deforms the Lax operators by

$$\delta Q = \epsilon S(d)\,, \qquad \delta P = \epsilon R(d)\,, \tag{A.22}$$

where $S(d)$ and $R(d)$ are polynomials in d of degree $p-2$ and $q-2$ respectively. Since this deformation must preserve the string equation $[P,Q] = \hbar$, this leads to the following constraint at linear order in ϵ:

$$[P, \delta Q] + [\delta P, Q] = 0\,. \tag{A.23}$$

Substituting (A.22) and using (A.21), we find

$$(P(d+r) - P(d))S(d) = (Q(d+r) - Q(d))R(d)\,. \tag{A.24}$$

This constraint must be satisfied for every d and for some constant r. Since $Q(d+r) - Q(d)$ and $P(d+r) - P(d)$ are degree $q-1$ and $p-1$ respectively, but $S(d)$ and $R(d)$ are only degree $p-2$ and $q-2$ respectively, (A.24) implies that $Q(d+r) - Q(d)$ and $P(d+r) - P(d)$ must share a common root. Thus there exists some $d = d_0$ where

$$(Q(d_0+r), P(d_0+r)) = (Q(d_0), P(d_0))\,. \tag{A.25}$$

The authors of [51] use (A.25) to solve for r, and then use (A.24) to solve for $S(d)$ and $R(d)$.

With the geometric interpretation of the previous sections in hand, we can offer some new insights into the analysis of the instantons. The condition (A.25) is equivalent to the condition that $\mathcal{M}_{p,q}$ have a singularity (pinched cycle) at the point $(x,y) = (Q(d_0), P(d_0))$.

This shows that the instantons are in one-to-one correspondence with the singularities of $\mathcal{M}_{p,q}$. It confirms in a direct way the analysis of [23] and the interpretation of the ZZ branes as instantons.

In [23], it was also argued that the period of $y\,dx$ around the B-cycle passing through the (m,n) singularity computes the (m,n) instanton (ZZ brane) action, i.e.

$$Z_{m,n} \propto \oint_{B_{m,n}} y\,dx = \int_{z_{m,n}}^{z_{m,n}+r_{m,n}} y(z)x'(z)dz \tag{A.26}$$

with the constant of proportionality independent of m and n. The derivative of this with respect to the lowest-dimension coupling τ must then be essentially the constant r defined in (A.20). Indeed, a calculation similar to (2.36) shows that

$$\partial_\tau Z_{m,n} \propto \int_{z_{m,n}}^{z_{m,n}+r_{m,n}} dz = r_{m,n} \tag{A.27}$$

as expected. This provides a non-trivial check of the formula (A.26) for the instanton actions derived in [23]. It also generalizes (and simplifies) the analysis of [40], where (A.27) was proven for the special case of the conformal background.

In the conformal background, one can check that the instanton actions $r_{m,n}$ are always real. However, in a general background they will be complex. For instance, in the $(2,2m-1)$ models perturbed by the lowest-dimension operator, one can use the formulas in [51] to prove this explicitly for m odd. When the $r_{m,n}$ are complex, the corresponding (p,q) minimal string theory is expected to be nonperturbatively consistent and Borel summable. In these cases, the $r_{m,n}$ come in conjugate pairs, so that even though they are complex, the total instanton correction to the partition function is real.

B. A brief review of Stokes' phenomenon

In this appendix we will briefly review Stokes' phenomenon, summarizing [39]. Consider the following integral

$$I(x) = \int_{\mathcal{C}_0} ds\; e^{-\frac{1}{\hbar}\mathcal{S}(s,x)}\,, \tag{B.1}$$

where $\mathcal{S}(s,x)$ is holomorphic in s, and $\mathcal{C}_0$ is a contour in the complex s-plane, chosen so that the integral exists and admits an analytic continuation to some region of the complex x-plane. We are interested in the $\hbar \to 0$ asymptotics. Since $\frac{\partial \mathcal{S}}{\partial \bar{s}} = 0$, lines of constant $\operatorname{Im}\mathcal{S}$ are perpendicular to lines of constant $\operatorname{Re}\mathcal{S}$; i.e. they are gradient lines of $\operatorname{Re}\mathcal{S}$. We would like to deform the contour $\mathcal{C}_0$ in (B.1) to a steepest descent contour $\mathcal{C}$ — a gradient line of $\operatorname{Re}\mathcal{S}$ along which $\operatorname{Im}\mathcal{S}$ is constant. (The latter requirement prevents cancellation between different non-saddle portions of the contour in the leading $\hbar \to 0$ approximation.) At a generic point such lines do not intersect. However, the saddle points $\frac{\partial \mathcal{S}}{\partial s} = 0$ are characterized by having two intersecting steepest descent lines.

Since typically the different saddle points occur at different values of $\operatorname{Im}\mathcal{S}$, it is impossible to deform the contour $\mathcal{C}_0$ to a steepest descent contour (constant $\operatorname{Im}\mathcal{S}$) $\mathcal{C}$ passing through all of them. However, if the steepest descent contours $\mathcal{C}_{1,2}$ through two different

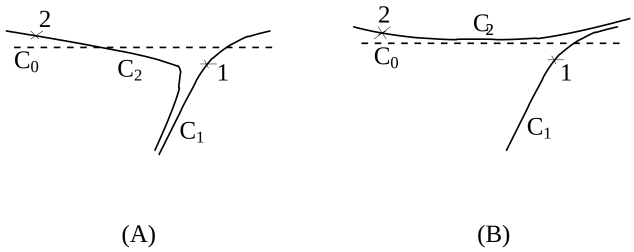

Figure 1: The steepest descent lines $\mathcal{C}_{1,2}$ pass through the saddles points 1 and 2. The dotted line is the original integration contour $\mathcal{C}_0$. For one value of x the situation is as in figure A, and $\mathcal{C}_0$ can be replaced by $\mathcal{C} = \mathcal{C}_1 + \mathcal{C}_2$ because the two contours $\mathcal{C}_1$ and $\mathcal{C}_2$ meet at an asymptotic infinity where the integrand vanishes. Then the integral receives contributions from the two saddles. For another value of x, as in figure B, the steepest descent contour is given by $\mathcal{C} = \mathcal{C}_2$ alone, and so the integral receives a contribution only from the saddle 2. The transition occurs for the values of x for which $\mathrm{Im}\,\mathcal{S}(1) = \mathrm{Im}\,\mathcal{S}(2)$.

saddles labelled by 1 and 2 pass near each other, and have the proper asymptotic behavior, we can deform $\mathcal{C}_0$ as follows. We deform it to a steepest descent contour $\mathcal{C}$ which starts close to $\mathcal{C}_1$ passes near the saddle point 1, then passes near the saddle point 2 and finishing close to $\mathcal{C}_2$. Such a contour must be compatible with the asymptotic behavior of the original contour $\mathcal{C}_0$. Alternatively, if $\mathcal{C}_1$ and $\mathcal{C}_2$ asymptote to each other at infinity and $\mathrm{Re}\,\mathcal{S} \to +\infty$ there, we can take $\mathcal{C} = \mathcal{C}_1 + \mathcal{C}_2$ (see figure 1 and the example below). This makes it clear that the two saddles contribute to the integral.

Now let us vary the parameter x in (B.1) and examine the saddles and the contour $\mathcal{C}$. There are two interesting things that can happen. The first, more trivial phenomenon is when the two saddles exchange dominance. This occurs across lines in the complex x plane called "anti-Stokes lines," where the values of $\mathrm{Re}\,\mathcal{S}$ at the two saddles are the same. The second, more interesting critical behavior happens across the "Stokes lines," where the values of $\mathrm{Im}\,\mathcal{S}$ at the two saddles are the same and the topology of $\mathcal{C}_{1,2}$ changes. Beyond this point the contour with the correct asymptotic behavior, or equivalently a smooth deformation of the previous contour $\mathcal{C}$, does not pass through the two saddles but only through one of them. It is possible to find another contour which passes through both of them, but it does not have the correct asymptotic behavior. The exchange of dominance of two saddles and the abrupt disappearance of the saddle-point contribution to the integral $I(x)$ both contribute to Stokes' phenomenon. As mentioned in the body of the paper, this is the phenomenon in which the analytic continuation of the asymptotic expansion of a function does not agree with the asymptotic expansion of the functions' analytic continuation.

As an example, consider the Airy function

$$\int_{-\infty}^{+\infty} ds e^{\frac{i}{\hbar}\left(\frac{s^3}{3}+xs\right)} \,. \tag{B.2}$$

The behavior as $|s| \to \infty$ allows us to deform the contour to start in the wedge $\frac{2\pi}{3} \leq \arg(s) \leq \pi$ and end in the wedge $0 \leq \arg(s) \leq \frac{\pi}{3}$. The two saddles at $s = \pm\sqrt{-x}$ are as in figure 1. There is an anti-Stokes line located on the negative x axis. Here the two saddles are purely imaginary (i.e. $\mathrm{Re}\,\mathcal{S}=0$) and they exchange dominance. One can also check that the lines $|\arg(x)|=\frac{2\pi}{3}$ are Stokes lines. Thus, figure A applies to $\frac{2\pi}{3}\le|\arg(x)|\le\pi$ and figure B applies to $0\le|\arg(x)|\le\frac{2\pi}{3}$. As one crosses the Stokes lines starting from the negative real axis, the dominant saddle ceases to contribute.

C. Numerical analysis of $(p,q)=(2,5)$

In this appendix we will analyze in detail the example of $(p,q)=(2,5)$, using numerical methods where necessary. The purpose of this analysis is mainly to verify that the lessons we learned from the example of $(2,1)$ indeed carry over to more complicated models.

To begin, we define the Lax operators to be

$$Q=d^2-u(\tau),\qquad P=\sum_{k=0}^{2}t_{2k+3}Q_+^{k+1/2}\,,\qquad d=\hbar\,\partial_\tau\,. \tag{C.1}$$

This describes a perturbation around the $(2,5)$ multi-critical point. Let us set $t_7=-8/5$ without loss of generality. Then the string equation $[P,Q]=\hbar$ takes the form

$$u^3+\frac{3}{4}t_5u^2-t_3u-\tau-\frac{1}{4}\hbar^2\left(2u'^2+4uu''+t_5u''\right)+\frac{1}{10}\hbar^4u^{(4)}=0\,. \tag{C.2}$$

The Baker-Akhiezer function is determined by the differential equations

$$Q\psi=x\psi\,,\qquad P\psi=\hbar\partial_x\psi\,, \tag{C.3}$$

together with the condition that ψ is real and exponentially decreasing as $x\to+\infty$.

Before we proceed to solve (C.2) and (C.3) numerically, let us first discuss the classical limit $\hbar\to0$. At $\hbar=0$, P and Q take the form

$$Q=d^2-u,\qquad P=-\frac{8}{5}d^5+(4u+t_5)d^3-\left(3u^2+\frac{3}{2}t_5u-t_3\right)d \tag{C.4}$$

with $u(\tau)$ the solution to (C.2) with $\hbar=0$. Therefore they lie on the Riemann surface described by the algebraic equation

$$P^2=\frac{1}{25}(Q+u)\left(8Q^2-4\left(u+\frac{5}{4}t_5\right)Q+3u^2+\frac{5}{2}t_5u-5t_3\right)^2\,. \tag{C.5}$$

Here we see explicitly how the Riemann surface takes the form (A.19) for all values of the closed-string couplings τ,t_3,t_5. In particular, the Riemann surface always has a branch point at $Q=-u$ and singularities at the other roots of the r.h.s. of (C.5). Therefore the KdV flows, which change the values of the closed string couplings, indeed correspond to singularity-preserving deformations of the Riemann surface.

Now let us discuss the numerical solution of the string equation (C.2) and the Baker-Akhiezer equations (C.3). The string equation for perturbations around the $(p,q)=(2,5)$ critical point was solved numerically in [47, 49]. Here we will repeat the analysis of [47, 49] to obtain the specific heat $u(\tau)$ for various values of $\hbar$. We will then take the analysis one

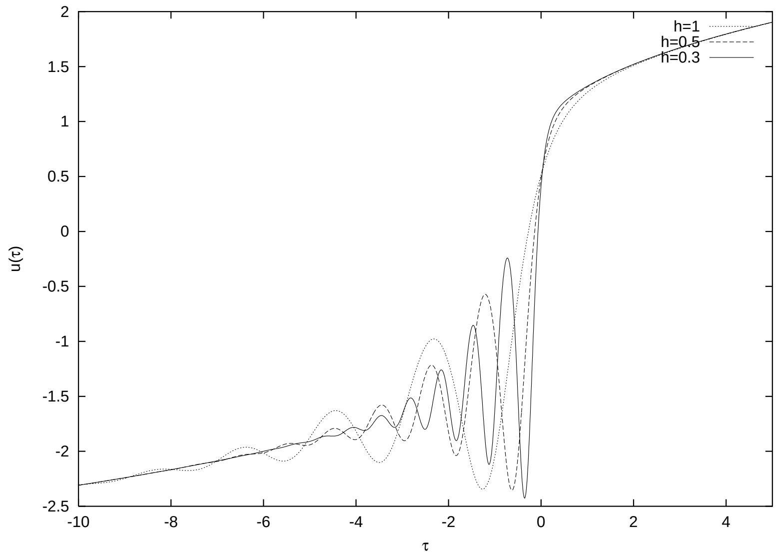

Figure 2: The specific heat $u(\tau)$ as a function of the lowest-dimension coupling τ, for $\hbar = 1, 0.5, 0.3$. These plots were obtained by numerically solving the string equation (C.2) in the conformal background (C.6).

step further by numerically solving (C.3) for the Baker-Akhiezer function. For simplicity, let us limit ourselves to the conformal background perturbed by the lowest-dimension operator. The conformal background corresponds to

$$\tau = 0\,, \qquad t_3 = 1\,, \qquad t_5 = 0\,. \tag{C.6}$$

Up to a trivial shift of u and τ this is identical to the setup considered in [49]. To see that this is the conformal background, simply substitute (C.6) into the formula (C.5) for the Riemann surface. Since the string equation (C.2) is solved by $u(\tau = 0) = 1$ (modulo a discrete choice for the root of the cubic polynomial) the curve becomes

$$y^2 = \frac{4}{25}(x+1)(4x^2 - 2x - 1)^2 \tag{C.7}$$

which is indeed the same as $T_2(y) = T_5(x)$ after a rescaling of y.

Shown in figure 2 is the specific heat $u(\tau)$ versus τ for various values of $\hbar$. At large $|\tau|$ the specific heat asymptotes to the classical solution $u_{\rm cl}(\tau) \sim \mathrm{sign}(\tau)|\tau|^{1/3}$. Meanwhile, at small $|\tau|$ the specific heat oscillates faster and faster as $\hbar$ is decreased, since here the function is trying increasingly hard to interpolate smoothly between the classical discontinuity $u_{\rm cl}(\tau = 0) = \pm 1$ at $\tau = 0$. Evidently, the classical limit of $u(\tau)$ is not well-defined for small $|\tau|$, although the quantum answer is smooth.

Figure 3 contains a plot of the Baker-Akhiezer function $\psi(x,t)$, again for various values of $\hbar$. (The different solutions have been rescaled in order to aid the presentation.) From the figure, it is clear that $\psi(x,t)$ is decreasing at large positive x, while it is oscillatory for $x < -1$. Also, the function is clearly always smooth and real-valued. The bump at $x \approx \frac{1+\sqrt{5}}{4}$ in figure 3 corresponds to the location of the $(1,2)$ ZZ brane, while the trough at

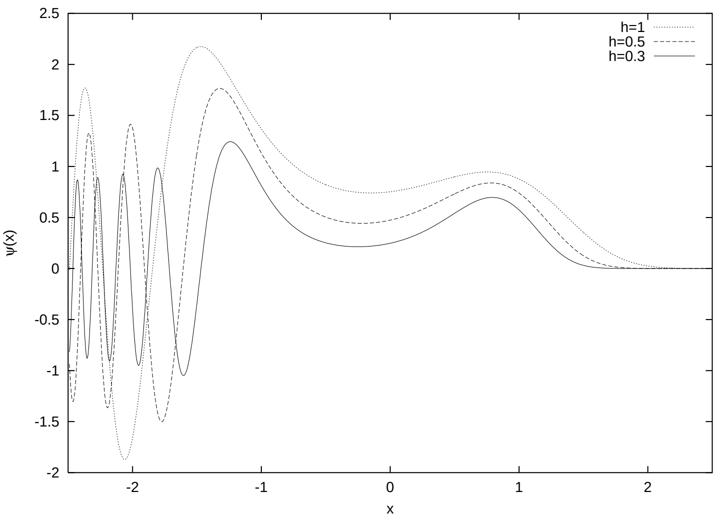

Figure 3: The Baker-Akhiezer function $\psi(x,t)$ versus the boundary cosmological constant x, for $\hbar = 1, 0.5, 0.3$. The plots have been rescaled for the different values of $\hbar$, so as to improve the presentation.

$x \approx \frac{1-\sqrt{5}}{4}$ is the location of the $(1,1)$ ZZ brane. As $\hbar$ decreases, the oscillations at $x < -1$ become faster, and the bump at $x \approx \frac{1+\sqrt{5}}{4}$ becomes more well-defined. This behavior is all qualitatively consistent with the leading-order WKB approximation

$$\psi_{\rm cl}(x,t) \approx \begin{cases} (-1-x)^{-1/4} e^{\int_{-1}^{x} y\, dx'/\hbar} & x > -1 \\ 2(x+1)^{-1/4} \sin\left(\frac{\pi}{4} - \frac{i}{\hbar}\int_{-1}^{x} y\, dx'\right) & x < -1\,, \end{cases} \tag{C.8}$$

where $y = y(x)$ is given by (C.7).

A more quantitative comparison between the WKB approximation and the exact answer is shown in figure 4, $\hbar = 0.3$. We see that they are in excellent agreement, except for a small region around $x = -1$ where we expect the WKB approximation to break down anyway.

It should be clear from the discussion that these numerical results confirm many of the general arguments in the text regarding the properties of the Baker-Akhiezer function $\psi(x,t)$. Let us just mention a few. First, $\psi(x,t)$ obviously exhibits Stokes' phenomenon: the analytic continuation of the asymptotics (C.8) away from large positive x, where $\psi(x,t)$ is exponentially decreasing, leads to the wrong answer for $x < -1$, where $\psi(x,t)$ is oscillatory. Second, notice that the analytic continuation of the WKB approximation from large positive x is accurate up until $x \approx -1$. The failure of the analytic continuation of the WKB approximation beyond $x = -1$ is due to the level crossing phenomenon, which results in the oscillatory behavior of $\psi(x,t)$. These facts agree well with the general discussion in section 2. Finally, note that the Baker-Akhiezer function is exponentially *decreasing* at large positive x. From section 5, we know that this is the expected behavior for the nonperturbatively consistent $(2,5)$ model.

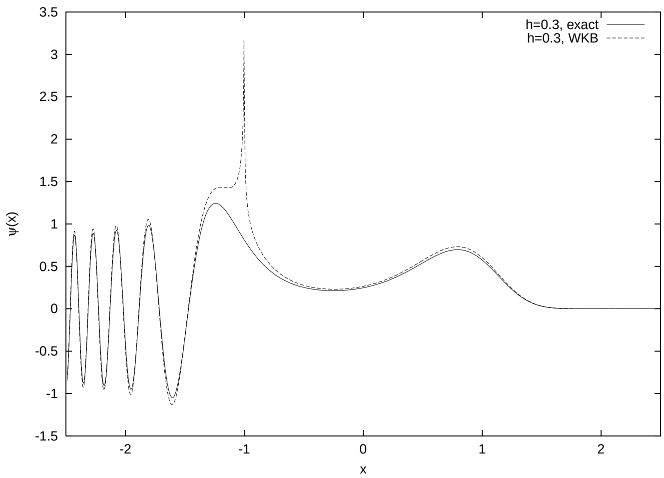

Figure 4: A comparison of exact Baker-Akhiezer function and its leading-order WKB approximation, for $\hbar = 0.3$. The two are clearly in excellent agreement, except in a small region around $x = -1$ where the WKB approximation is expected to break down.

References

[1] F. David, *Planar diagrams, two-dimensional lattice gravity and surface models*, *Nucl. Phys.* **B 257** (1985) 45.

[2] V.A. Kazakov, *Bilocal regularization of models of random surfaces*, *Phys. Lett.* **B 150** (1985) 282.

[3] V.A. Kazakov, A.A. Migdal and I.K. Kostov, *Critical properties of randomly triangulated planar random surfaces*, *Phys. Lett.* **B 157** (1985) 295.

[4] J. Ambjørn, B. Durhuus and J. Fröhlich, *Diseases of triangulated random surface models and possible cures*, *Nucl. Phys.* **B 257** (1985) 433.

[5] M.R. Douglas and S.H. Shenker, *Strings in less than one-dimension*, *Nucl. Phys.* **B 335** (1990) 635.

[6] D.J. Gross and A.A. Migdal, *Nonperturbative two-dimensional quantum gravity*, *Phys. Rev. Lett.* **64** (1990) 127.

[7] E. Brezin and V.A. Kazakov, *Exactly solvable field theories of closed strings*, *Phys. Lett.* **B 236** (1990) 144.

[8] M.R. Douglas, *Strings in less than one-dimension and the generalized K-D-V hierarchies*, *Phys. Lett.* **B 238** (1990) 176.

[9] P.H. Ginsparg and G.W. Moore, *Lectures on 2D gravity and 2D string theory*, `hep-th/9304011`.

[10] P. Di Francesco, P.H. Ginsparg and J. Zinn-Justin, *2D gravity and random matrices*, *Phys. Rept.* **254** (1995) 1 [`hep-th/9306153`].

[11] H. Dorn and H.J. Otto, *Some conclusions for noncritical string theory drawn from two and three point functions in the Liouville sector*, `hep-th/9501019`.

[12] A.B. Zamolodchikov and A.B. Zamolodchikov, *Structure constants and conformal bootstrap in Liouville field theory*, *Nucl. Phys.* **B 477** (1996) 577 [hep-th/9506136].

[13] J. Teschner, *On the Liouville three point function*, *Phys. Lett.* **B 363** (1995) 65 [hep-th/9507109].

[14] V. Fateev, A.B. Zamolodchikov and A.B. Zamolodchikov, *Boundary liouville field theory, I. Boundary state and boundary two-point function*, hep-th/0001012.

[15] J. Teschner, *Remarks on Liouville theory with boundary*, hep-th/0009138.

[16] A.B. Zamolodchikov and A.B. Zamolodchikov, *Liouville field theory on a pseudosphere*, hep-th/0101152.

[17] B. Ponsot and J. Teschner, *Boundary Liouville field theory: boundary three point function*, *Nucl. Phys.* **B 622** (2002) 309 [hep-th/0110244].

[18] J. McGreevy and H. Verlinde, *Strings from tachyons: the $c = 1$ matrix reloaded*, *J. High Energy Phys.* **12** (2003) 054 [hep-th/0304224].

[19] E.J. Martinec, *The annular report on non-critical string theory*, hep-th/0305148.

[20] I.R. Klebanov, J. Maldacena and N. Seiberg, *D-brane decay in two-dimensional string theory*, *J. High Energy Phys.* **07** (2003) 045 [hep-th/0305159].

[21] J. McGreevy, J. Teschner and H. Verlinde, *Classical and quantum D-branes in 2D string theory*, *J. High Energy Phys.* **01** (2004) 039 [hep-th/0305194].

[22] I.R. Klebanov, J. Maldacena and N. Seiberg, *Unitary and complex matrix models as 1D type 0 strings*, hep-th/0309168.

[23] N. Seiberg and D. Shih, *Branes, rings and matrix models in minimal (super)string theory*, *J. High Energy Phys.* **02** (2004) 021 [hep-th/0312170].

[24] D. Gaiotto and L. Rastelli, *A paradigm of open/closed duality: Liouville D-branes and the Kontsevich model*, hep-th/0312196.

[25] M. Hanada et al., *Loops versus matrices: the nonperturbative aspects of noncritical string*, *Prog. Theor. Phys.* **112** (2004) 131 [hep-th/0405076].

[26] D. Kutasov, K. Okuyama, J.W. Park, N. Seiberg and D. Shih, *Annulus amplitudes and ZZ branes in minimal string theory*, *J. High Energy Phys.* **08** (2004) 026 [hep-th/0406030].

[27] J. Ambjørn, S. Arianos, J.A. Gesser and S. Kawamoto, *The geometry of ZZ-branes*, hep-th/0406108.

[28] T. Banks, W. Fischler, S.H. Shenker and L. Susskind, *M-theory as a matrix model: a conjecture*, *Phys. Rev.* **D 55** (1997) 5112 [hep-th/9610043].

[29] G.W. Moore, N. Seiberg and M. Staudacher, *From loops to states in 2D quantum gravity*, *Nucl. Phys.* **B 362** (1991) 665.

[30] J.M. Daul, V.A. Kazakov and I.K. Kostov, *Rational theories of 2D gravity from the two matrix model*, *Nucl. Phys.* **B 409** (1993) 311 [hep-th/9303093].

[31] T. Banks, M.R. Douglas, N. Seiberg and S.H. Shenker, *Microscopic and macroscopic loops in nonperturbative two-dimensional gravity*, *Phys. Lett.* **B 238** (1990) 279.

[32] G.W. Moore and N. Seiberg, *From loops to fields in 2D quantum gravity*, *Int. J. Mod. Phys.* **A 7** (1992) 2601.

[33] I.K. Kostov, *Multiloop correlators for closed strings with discrete target space*, *Phys. Lett.* **B 266** (1991) 42.

[34] A. Morozov, *Integrability and matrix models*, *Phys. Usp.* **37** (1994) 1–55 [hep-th/9303139].

[35] G.W. Moore, *Matrix models of 2D gravity and isomonodromic deformation*, *Prog. Theor. Phys. Suppl.* **102** (1990) 255

[36] G.W. Moore, *Geometry of the string equations*, *Commun. Math. Phys.* **133** (1990) 261.

[37] L. Fidkowski, V. Hubeny, M. Kleban and S. Shenker, *The black hole singularity in AdS/CFT*, *J. High Energy Phys.* **02** (2004) 014 [hep-th/0306170].

[38] M. Aganagic, R. Dijkgraaf, A. Klemm, M. Marino and C. Vafa, *Topological strings and integrable hierarchies*, hep-th/0312085.

[39] M.V. Berry, *Stokes' phenomenon smoothing a victorian discontinuity*, *Inst. Hautes Études Sci. Publ. Math.* **68** (1988) 211.

[40] V.A. Kazakov and I.K. Kostov, *Instantons in non-critical strings from the two-matrix model*, hep-th/0403152.

[41] P. Bleher and A. Its, *Double scaling limit in the random matrix model: the Riemann-Hilbert approach*, math.ph/0201003.

[42] R. Dijkgraaf, *Intersection theory, integrable hierarchies and topological field theory*, hep-th/9201003.

[43] I.K. Kostov, *Conformal field theory techniques in random matrix models*, hep-th/9907060.

[44] F. David, *Phases of the large-N matrix model and nonperturbative effects in 2D gravity*, *Nucl. Phys.* **B 348** (1991) 507.

[45] I.R. Klebanov and E. Witten, *AdS/CFT correspondence and symmetry breaking*, *Nucl. Phys.* **B 556** (1999) 89 [hep-th/9905104].

[46] R. Dijkgraaf, A. Sinkovics and M. Temurhan, *Universal correlators from geometry*, hep-th/0406247.

[47] E. Brezin, E. Marinari and G. Parisi, *A nonperturbative ambiguity free solution of a string model*, *Phys. Lett.* **B 242** (1990) 35.

[48] F. David, *Loop equations and nonperturbative effects in two-dimensional quantum gravity*, *Mod. Phys. Lett.* **A 5** (1990) 1019.

[49] M.R. Douglas, N. Seiberg and S.H. Shenker, *Flow and instability in quantum gravity*, *Phys. Lett.* **B 244** (1990) 381.

[50] G. Segal and G. Wilson, *Loop groups and equations of KdV type*, *Publ. IHES* **61** (1985) 1.

[51] B. Eynard and J. Zinn-Justin, *Large order behavior of 2D gravity coupled to D ¡ 1 matter*, *Phys. Lett.* **B 302** (1993) 396 [hep-th/9301004].